UNIVERSITEIT VAN PRETORIA
UNIVERSITY OF PRETORIA
YUNIBESITHI YA PRETORIA

Exploring the mode of action of MMV1580843 against *Plasmodium falciparum*

By Dana Caitlin Schultz

17031983

Submitted in fulfilment of the requirements for the degree

Magister Scientiae in Biochemistry

in the Faculty of Natural and Agricultural Sciences

Department of Biochemistry, Genetics and Microbiology
Division of Biochemistry

University of Pretoria

December 2023

UNIVERSITEIT VAN PRETORIA
UNIVERSITY OF PRETORIA
YUNIBESITHI YA PRETORIA

Submission Declaration

I, Dana Caitlin Schultz, declare that the dissertation, which I hereby submit for the degree *Magister Scientiae* in the Department of Biochemistry, Genetics, and Microbiology at the University of Pretoria, is my own work and has not previously been submitted by me for a degree at this or any other tertiary institution.

Signature: 

Date: December 2023

Declaration of Originality

University of Pretoria

Faculty of Natural and Agricultural Sciences

Department of Biochemistry, Genetics, and Microbiology

Full names of student: **Dana Caitlin Schultz**

Student number: **17031983**

Declaration

1. I understand what plagiarism is and am aware of the University's policy in this regard.

2. I declare that this dissertation is my original work. Where other people's work has been used (either from a printed source, Internet, or any other source), this has been properly acknowledged and referenced in accordance with requirements.

3. I have not used work previously produced by another student or any other person to hand in as my own.

4. I have not allowed and will not allow anyone to copy my work with the intention of passing it off as his or her own.

Signature: 

Date: December 2023

Acknowledgements

This dissertation is dedicated to my mother and father, Karen and Barry Schultz, and my fiancé, Tristan Little.

I extend my deepest gratitude to my mother, whose unwavering support, countless sacrifices, and encouragement have been the cornerstone of my academic journey. She is an inspiration to me and none of this would have been possible without her constant belief in my abilities. In honour of the lasting impact my father has on my life, I dedicate this dissertation to his memory.

I am profoundly thankful to my fiancé for standing by my side and being a constant source of encouragement throughout all the highs and lows. His belief in me, as well as his continual investment in my studies and successes, has been a driving force throughout this journey.

Special thanks to my siblings, Gregory, Jeffery and Caroline Schultz, my stepdad, John Petrie, and my closest friends for their understanding and support which made this academic pursuit a richer experience.

To the M^2PL members, I express my appreciation for their willingness to share knowledge and offer assistance. A heartfelt thanks to Dr Michelle Kok and Daniel Opperman, whose contributions played a crucial role in the success of this dissertation. My sincere gratitude to Shanté da Rocha for generously providing the asexual parasites needed for completing my lab work. To my former supervisor on this project, Dr Janette Reader, a special thanks for all the assistance and guidance during the first year of my masters.

I extend my appreciation to my fellow master's students in my year – Christea van Zyl, Sizwe Tshabalala, Jean Thomas, Marché Maré, and Martha Murya – for making the challenges of postgraduate studies more bearable.

I would like to acknowledge the Bill and Melinda Gates Foundation through the Grand Challenges Africa Drug Discovery programme – managed by the Science for Africa Foundation, the NRF SARChI - DSI/NRF SARChI (UID 84627) and MRC SHIP for funding this degree.

Finally, my sincere gratitude and thanks go to my supervisor, Dr Mariëtte van der Watt, and co-supervisor, Professor Lyn-Marie Birkholtz, for their invaluable mentorship, guidance, support and expertise throughout the completion of my dissertation.

Table of Contents

List of Figures

List of Tables

List of Abbreviations

ABS	Asexual blood stage
ACTs	Artemisinin-based combination therapies
CB1	Cannabinoid receptor-1
CQ	Chloroquine
ER	Endoplasmic reticulum
FV	Food vacuole
IMC	Inner membrane complex
IVIEWGA	*In vitro* evolution and whole-genome analysis
iRBCs	Infected red blood cells
IRS	Indoor residual spraying
ITNs	Insecticide-treated nets
MmpL3	Mycobacterial membrane protein, large
MMV	Medicines for Malaria Venture
MoA	Mode of action
NAG	*N*-acetyl glucosamine
OXPHOS	Oxidative phosphorylation
PI4K	Phosphatidylinositol 4-kinase
PRB	Pandemic Response Box
PVM	Parasitophorous vacuolar membrane
RBCs	Red blood cells
RND	Resistance nodulation-division
SEA	Similarity ensemble approach
SMILES	Simplified molecular input line entry system
SP	Sulfadoxine/pyrimethamine
TCPs	Target candidate profiles
TPPs	Target product profiles
WHO	World Health Organization

Summary

Although malaria is both preventable and curable, it is a parasitic disease with the highest fatality rate in history, causing over half a million deaths worldwide each year, with 95 % of the cases occurring in Africa. Female *Anopheles* mosquitoes act as vectors for the malaria parasite. *Plasmodium* is transmitted to a human host when a female *Anopheles* mosquito feeds on the individual. In turn, humans infected with the malaria parasite can transmit the parasite back to another mosquito, perpetuating the parasite's life cycle. The presence of both insecticide and therapeutic drug resistance to current antimalarials is an ongoing threat. Therefore, it is crucial that the next generation of antimalarials include compounds with unique modes of action and exhibiting high barriers to resistance development. Blocking transmission is essential for malaria elimination, given that current drugs primarily target asexual parasites or sporozoites and liver stages. The lower number and non-replicating nature of gametocytes render the development of resistance to transmission-blocking antimalarials highly improbable. Gametocyte-specific antimalarials are presumed to target unique biological processes compared to compounds targeting asexual parasites, reflecting the fundamental difference in the biology associated with asexual proliferation and gametocyte differentiation. A key drawback of phenotypic screening of candidate antimalarials is the lack of knowledge regarding the mode of action of a compound, which is the bottleneck of drug discovery and development. While current target identification strategies predominantly focus on the asexual stages of the parasite life cycle, there is a noticeable gap in knowledge regarding the mode of action of gametocyte-specific antimalarials.

MMV1580843, a unique chemotype, is a structurally diverse and potent transmission-blocking compound, showing stage-specific activity towards non-proliferative gametocytes. This TCP-5 (target candidate profile-5, transmission-blocking) selective compound, with a potential novel mode of action in *Plasmodium*, was investigated here. This project thus aimed to determine the mode of action of MMV1580843 against *P. falciparum* late-stage gametocytes through biochemical approaches. The findings presented in this study point towards the mitochondria of late-stage gametocytes being the target of MMV1580843, supported by investigations involving fluorescent indicators and cross-reactivity with antimalarials having confirmed modes of action.

The results of this research exhibit a promising step forward in elucidating the mode of action of a gametocyte-specific antimalarial, providing a foundation for the development of targeted interventions to disrupt malaria transmission. By bridging the existing gap in knowledge and proposing an innovative strategy, this study contributes to the ongoing efforts in the global fight against malaria.

1. Literature Review

1.1. The effect of malaria worldwide

Malaria is a mosquito-borne infectious disease caused by intracellular protozoan parasites of the *Plasmodium* genus [1]. *Plasmodia* are obligate unicellular parasites and thus require a human host to complete their life cycle. Female *Anopheles* mosquitoes act as vectors for the malaria parasite. *Plasmodium spp.* is transmitted to a human host when a female *Anopheles* mosquito feeds on the individual. In turn, humans infected with the malaria parasite can transmit the parasite back to another mosquito, perpetuating the parasite's life cycle [2]. There are six species belonging to the *Plasmodium* genus which are responsible for causing various severities of the disease in humans, namely, *Plasmodium falciparum*, *Plasmodium vivax*, *Plasmodium malariae*, *Plasmodium ovale*, *Plasmodium knowlesi* and *Plasmodium cynomolgi* [3, 4]. Of these six *Plasmodium* species, *P. falciparum* and *P. vivax* are the most life-threatening. Nearly half of the world's population resides in malaria-endemic areas. Malaria takes its greatest toll primarily in subtropical and tropical regions, with sub-Saharan Africa being most severely affected by the disease (Figure 1.1) [5]. In fact, in 2021, the World Health Organization (WHO) reported the African region to account for 95 % of all malaria cases and 96 % of all deaths worldwide [6].

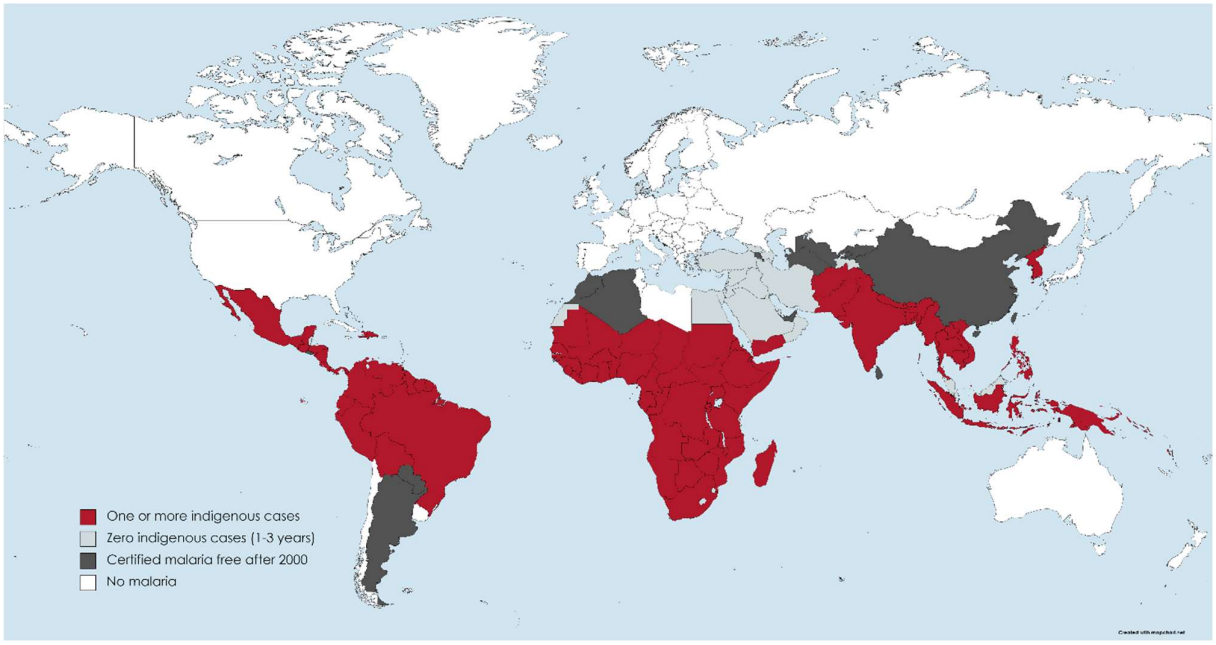

Figure 1.1: Distribution of Malaria incidence worldwide in 2021. Malaria takes its greatest toll primarily in the subtropical and tropical regions (indicated in maroon), with sub-Saharan Africa being most severely affected by the disease. Figure constructed in MapChart (https://www.mapchart.net/) and adapted from the WHO Malaria Report 2022 [6].

P. falciparum is the dominant species on the African continent [7] whereas, in most areas outside of sub-Saharan Africa, *P. vivax* is the most prevalent malaria parasite [6]. Although malaria is both

preventable and curable, it is the parasitic disease with the highest fatality recorded in history. In 2021, approximately 247 million people were infected worldwide, with an estimated 619 000 deaths [6]. Those most affected by the malaria parasite are children under the age of five, accounting for approximately 76 % of the deaths, who have only built-up partial immunity or no immunity at all, as well as individuals with HIV/AIDS [6]. Pregnant women are also more vulnerable to malaria as pregnancy decreases any previous immunity [8].

The severity of the *Plasmodium* infection differs by species and host parameters, including the degree of host immunity, which correlates to the prior level of parasite exposure [9, 10]. Malaria is commonly categorized as either asymptomatic, uncomplicated, or complicated/severe. In an individual, symptoms including fever cycles, nausea, chills, anaemia, headaches, sweating, diarrhoea and vomiting usually present themselves 7-10 days after a mosquito bite. These symptoms make diagnosis difficult due to their initial mild and non-specific nature. Severe (complicated) malaria, of which *P. falciparum* is the main aetiological agent, is life-threatening and typically presents with varied hallmarks of end-organ damage and severe anaemia [11]. Malaria is a treatable disease if detected and diagnosed in the early stages; however, it can progress to severe illness and is fatal if not treated in time.

1.2. *Plasmodium falciparum* parasite life cycle

The malaria parasite's life cycle is complex, comprising of many stages involving a human host and a mosquito vector (Figure 1.2). The sexual reproduction of the parasites' life cycle takes place in the *Anopheles* mosquito, while the asexual phase occurs in the liver (asymptomatic infection) and the red blood cells (RBCs, symptomatic infection) of the human host [5].

When a malaria-infected female *Anopheles* mosquito takes a blood meal from a human, *P. falciparum* sporozoites, located in the mosquito's salivary glands, are injected into the human host. Once the sporozoites are injected, they travel through the bloodstream and invade hepatocytes in the liver, initiating the asymptomatic exoerythrocytic developmental stage [12]. The sporozoites then repeatedly divide and differentiate asexually into hepatic schizonts that contain thousands of haploid merozoites (Figure 1.2A). After 10-14 days of development, the schizonts rupture, releasing merozoites into the bloodstream to infect RBCs and initiate the symptomatic, intraerythrocytic stage. In *P. ovale* and *P. vivax*, some sporozoites will not differentiate but remain dormant in a uninucleated stage, known as hypnozoites. Several weeks may pass before the hypnozoites resume replication [13].

Once the *P. falciparum* parasites have entered the RBCs, the invading merozoite matures from ring to trophozoite stage to finally form new schizonts after asexual cell replication and division (Figure 1.2B) [2]. After RBC rupturing, daughter merozoites are released, which will invade new RBCs again, reinitiating further asexual blood stage (ABS) replication cycles. Some merozoites may be destroyed

by the immune system; however, many invade RBCs immediately, allowing new schizonts to develop and mature. Furthermore, *Plasmodium* parasites also evade the immune system by expressing variant antigens on the surface of parasite-infected RBCs (iRBCs), which aid in cytoadherence to the endothelial lining to avoid splenic clearance [5, 14]. This all contributes to the pathology and disease symptoms associated with the disease.

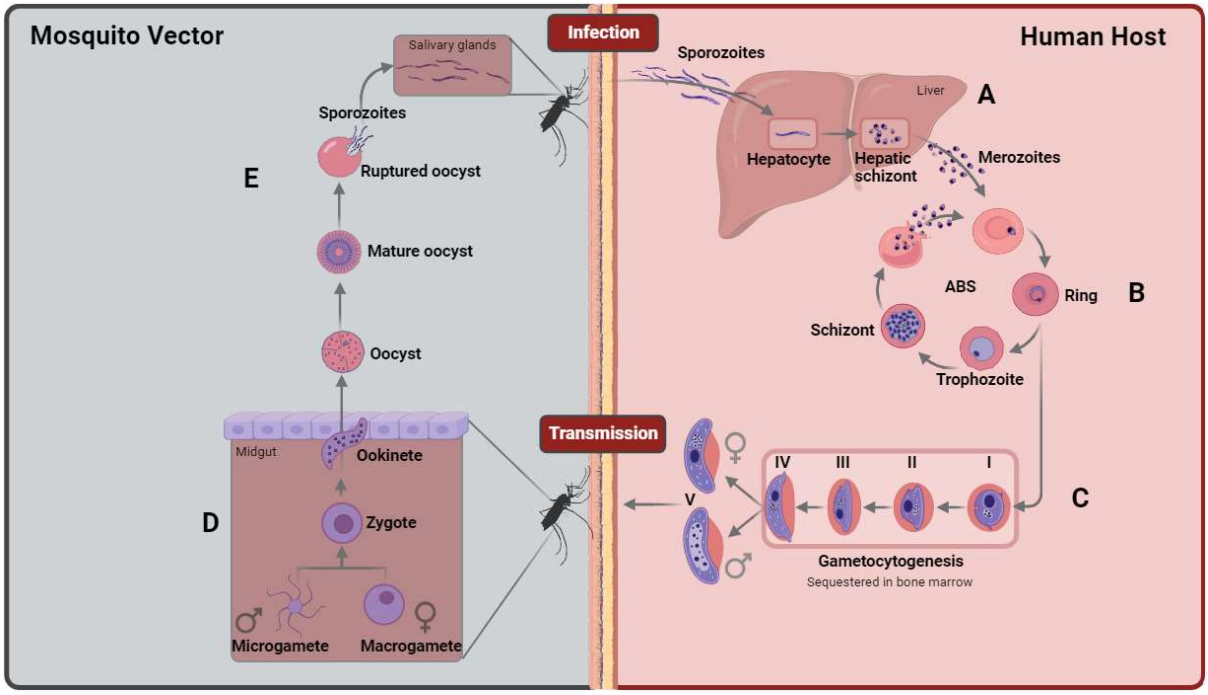

Figure 1.2: Life cycle of the *Plasmodium falciparum* malaria parasite. Injection of sporozoites from an infected female *Anopheles* mosquito initiates the malaria infection in humans. **A.** Sporozoites migrate to the liver and invade hepatocytes. The sporozoites replicate, forming schizonts which release thousands of merozoites into the bloodstream upon rupture. **B.** Merozoites then invade RBCs, undergo asexual replication and result in daughter merozoites being released, which invade new RBCs, reinitiating further ABS cycles. **C.** After numerous ABS cycles, a small percentage of the blood stage merozoites will undergo sexual differentiation resulting in mature stage V gametocytes. **D.** These gametocytes are ingested by another mosquito vector and begin to mature into male and female gametes. **E.** Fertilization occurs and the zygote replicates until sporozoites are formed. The sporozoites relocate to the salivary glands of the *Anopheles* mosquito, ready to infect a new human host and perpetuate the life cycle of the *P. falciparum* malaria parasite. Adapted from Lee et al., 2014 [2]. The image was created using BioRender.com under the basic license for educational purposes and basic design.

A small percentage of the ABS merozoites will differentiate into mosquito-transmissible sexual forms known as gametocytes. Both male and female gametocytes are produced through a process known as gametocytogenesis (Figure 1.2C). During gametocytogenesis, *P. falciparum* gametocytes mature through five morphological stages [15] and this process takes ~12 days, a timeframe unique to this parasite species. Stages I-IV are sequestered in the bone marrow of the host [16], whereas differentiated, mature stage V gametocytes are released into the bloodstream, taking 2-3 days before becoming infectious to mosquitoes [15].

An *Anopheles* mosquito ingests mature gametocytes from a human host upon feeding. The gametocytes differentiate into gametes in the mosquito midgut. The male gametocytes develop into motile male microgametes, while the female gametocytes round up, forming macrogametes (Figure 1.2D) [17]. After fertilization, motile zygotes are formed that then develop into ookinetes. The ookinetes then invade the mosquitoes' midgut wall, eventually developing into oocysts in which haploid sporozoites are formed. Sporozoites are released and migrate to the salivary glands of the *Anopheles* mosquito, ready to infect a new human host and perpetuate the life cycle of the *P. falciparum* malaria parasite (Figure 1.2E) [18].

1.3. Malaria control

1.3.1. Vector control

Reducing the transmission of the *Plasmodium* parasite through vector control measures is of utmost importance to decrease the number of malaria-associated morbidities and mortalities. Two of the most successful vector control interventions include indoor residual spraying (IRS) and insecticide-treated bednets (ITNs) [19]. ITNs provide a protective barrier between humans and mosquitoes, and are lethal to mosquitoes as they contain insecticides. Pyrethroids and pyrroles are the two classes of insecticides approved for use on ITNs as they can kill mosquitoes but do not pose major health risks to humans [8]. IRS is another intervention for the reduction of malaria transmission. IRS involves spraying certain insecticides (commonly dichlorodiphenyltrichloroethane (DDT)) on walls and surfaces where vectors are most likely to rest between bloodmeals. Both ITNs and IRS vector control strategies have greatly reduced malaria transmission; however, in more recent years, the emergence of insecticide resistance among *Anopheles* mosquitoes has become more prevalent. Despite the increase in vector resistance to pyrethroids, ITNs still provide some protection against malaria transmission [6]. However, a shift to non-pyrethroids has been observed in Africa due to pyrethroid resistance in mosquito vectors [20].

1.3.2. Parasite control by vaccination and antimalarial drugs

For decades, the complexity of the malaria parasites' life cycle, which involves a series of distinctive differentiation stages marked by specific proteins and host immune system targets [21], has posed a significant obstacle for immunologists and vaccinologists [22]. The first approved vaccine against *P. falciparum* is the pre-erythrocytic vaccine RTS,S/AS01, developed by GlaxoSmithKline. Malaria vaccines designed for the pre-erythrocytic phase focus on the *Plasmodium* parasite during its sporozoite and liver stages, to effectively halt its advancement to the blood stage [23]. Since October 2021, WHO has recommended that children living in areas with moderate to high malaria transmission receive the RTS,S/AS01 malaria vaccine [6]. RTS,S/AS01 works by blocking circumsporozoite proteins found on sporozoites' surfaces, to prevent development within the liver [24]. This recombinant vaccine is only 36 % effective after four treatments in children 5-17 months

of age [25]. A new vaccine, R21/Matrix-M, developed by Oxford, is the first vaccine to exceed the WHO-specified target of ≥75 % efficacy [25]. In October 2023, the WHO recommended this pre-erythrocytic vaccine to protect children against malaria.

Given the complexity of the *Plasmodium* parasite, a multifaceted approach is essential in the global fight against malaria. Although vector control strategies and vaccines are invaluable, chemotherapeutics are essential in treatment and prophylaxis, providing a first line of defence against the parasite. Directly targeting the parasite within the human host through chemotherapeutic agents complements the preventative benefits of vaccines and vector control strategies, thus mitigating the burden of malaria on at-risk populations.

P. falciparum, the species responsible for most malaria deaths, has developed resistance against almost all antimalarial therapeutics in existence [26]. This includes artemisinin-based combination therapies (ACTs), chloroquine (CQ), mefloquine, sulfadoxine/pyrimethamine and atovaquone. Between 2000 and 2015, malaria-associated deaths were reduced by an estimated 37 %; this was largely due to the increased availability and use of ACTs [12]. For uncomplicated malaria, ATCs are currently the first-line treatment [27], but the emergence of resistance has created a major cause for concern [28]. Hence, there is an urgent need for a new generation of antimalarials to overcome resistance to the current antimalarial chemotherapies, treat malaria-infected humans, control the mosquito vector, and block transmission by killing gametocytes [29]. Blocking transmission is essential for malaria elimination since current drugs, which either target sporozoites and liver stages or ABS parasites, only protect against individuals becoming infected or lower the severity of the clinical infection, respectively [30]. Therefore, attention has been shifted to transmission-blocking drugs to prevent the spread of the parasite and eliminate the risk of infection [31].

1.4. Discovering new antimalarial candidates

The discovery and development of new antimalarial drugs have been clearly defined by therapeutic application according to Medicines for Malaria Venture (MMV) guidelines [32]. These goals for new antimalarials are outlined by target candidate profiles (TCPs), describing the individual molecules, and target product profiles (TPPs), describing the final drug formulation containing TCP combinations [33]. TPPs are vital tools to guide novel antimalarial discovery and development, describing the minimally acceptable and ideal drug profile [34]. TPP-1 defines case management and TPP-2 chemoprotection. For TPP-1, the final drug formulation will contain two or more molecule combinations with activity against symptom-causing ABS parasites (TCP-1), gametocytes to block transmission (TCP-5) and molecules that target hypnozoites to prevent relapse (TCP-3) (Figure 1.3) [35]. TPP-2 will be given to individuals travelling to malaria-endemic areas or populations at risk from epidemics. The final drug formulation may include molecules with TCP-4 activity (targeting hepatic schizonts) and TCP-1 schizonticide activity (Figure 1.3) [35].

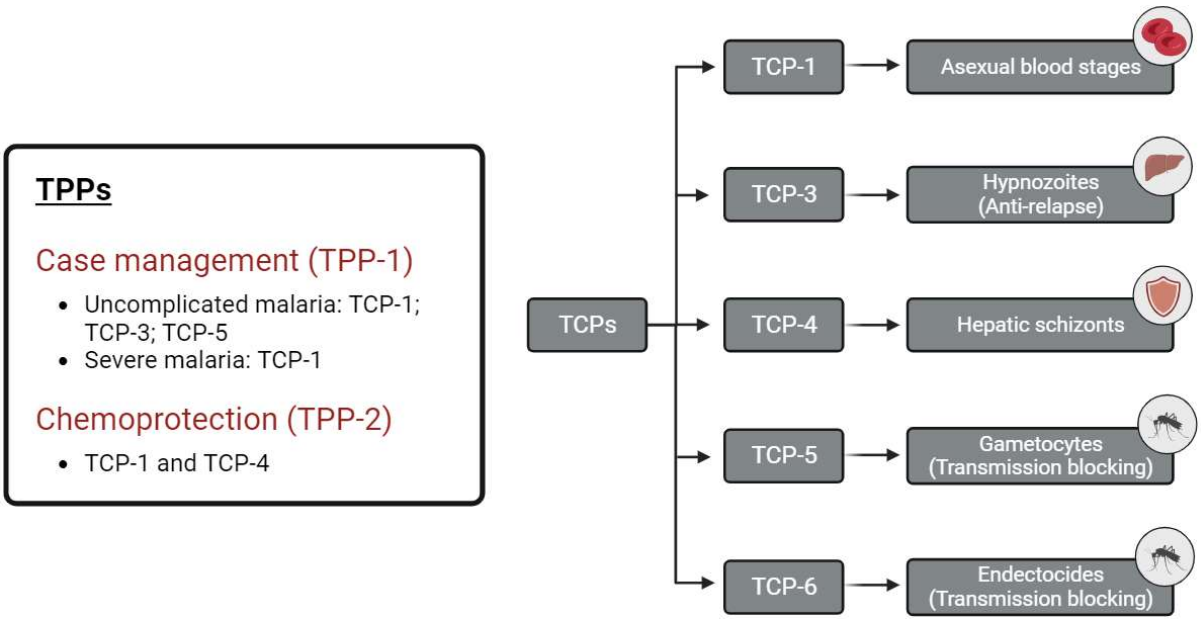

Figure 1.3: Target candidate profiles (TCP), describing individual molecules, and target product profiles (TPP), describing the final drug formulation. TPP-1 is used for case management, treating acute uncomplicated malaria in both adults and children, as well as severe malaria. TPP-2 is used for chemoprotection, administered to individuals migrating to high endemic areas or in the case of an epidemic. TCP-1: molecules which clear ABS parasitaemia; TCP-3: molecules having activity against dormant liver-stage hypnozoites (mainly *P. vivax*); TCP-4: molecules having activity against hepatic schizonts; TCP-5: molecules which block transmission by targeting parasite gametocytes; TCP-6: molecules which block transmission by targeting the insect vector. Adapted from Burrows *et al*., 2013 [34] and MMV [35]. The image was created using BioRender.com under the basic license for educational purposes and basic design.

Since many current antimalarials exclusively target ABS parasites as TCP-1 candidates, the development of new antimalarials that additionally target other stages, such as TCP-5 and TCP-4 candidates, is necessary [36]. In addition to targeting gametocytes, targeting alternative parasitic stages in mosquitoes could aid in reducing malaria transmission [37]. However, a considerable drawback of this approach is the indirect manner in which antimalarials are delivered since the antimalarial is required to remain at an effective concentration in the host's bloodstream for an extended time [38]. Furthermore, studies on drug targets in the sporogonic stages occurring in the mosquito are lacking [39]. Lastly, TCP-6 dictates the compounds should be able to kill the mosquito as endectocides, taken up in a blood meal and delivered through a mammalian host.

In recent years, new generations of antimalarials with novel modes of action (MoA) have made their way through the drug discovery and development pipeline, and have entered clinical development [34]. Typically, most of these antimalarials do not possess transmission-blocking effects and are ineffective in preventing infection, which is crucial when it comes to eliminating malaria [40]. Figure 1.4 lists the MMV-approved and currently-used antimalarials, as well as those under development, highlighting their TCPs. This list is updated regularly on the MMV website [41]. Asymptomatic carriers and those treated with the current antimalarials may still harbour gametocytes, which can be taken up by a mosquito vector during a blood meal, completing the malaria life cycle and sustaining the

burden of malaria. Drug discovery of a new generation of antimalarials emphasises blocking disease transmission and curing individual patients [42].

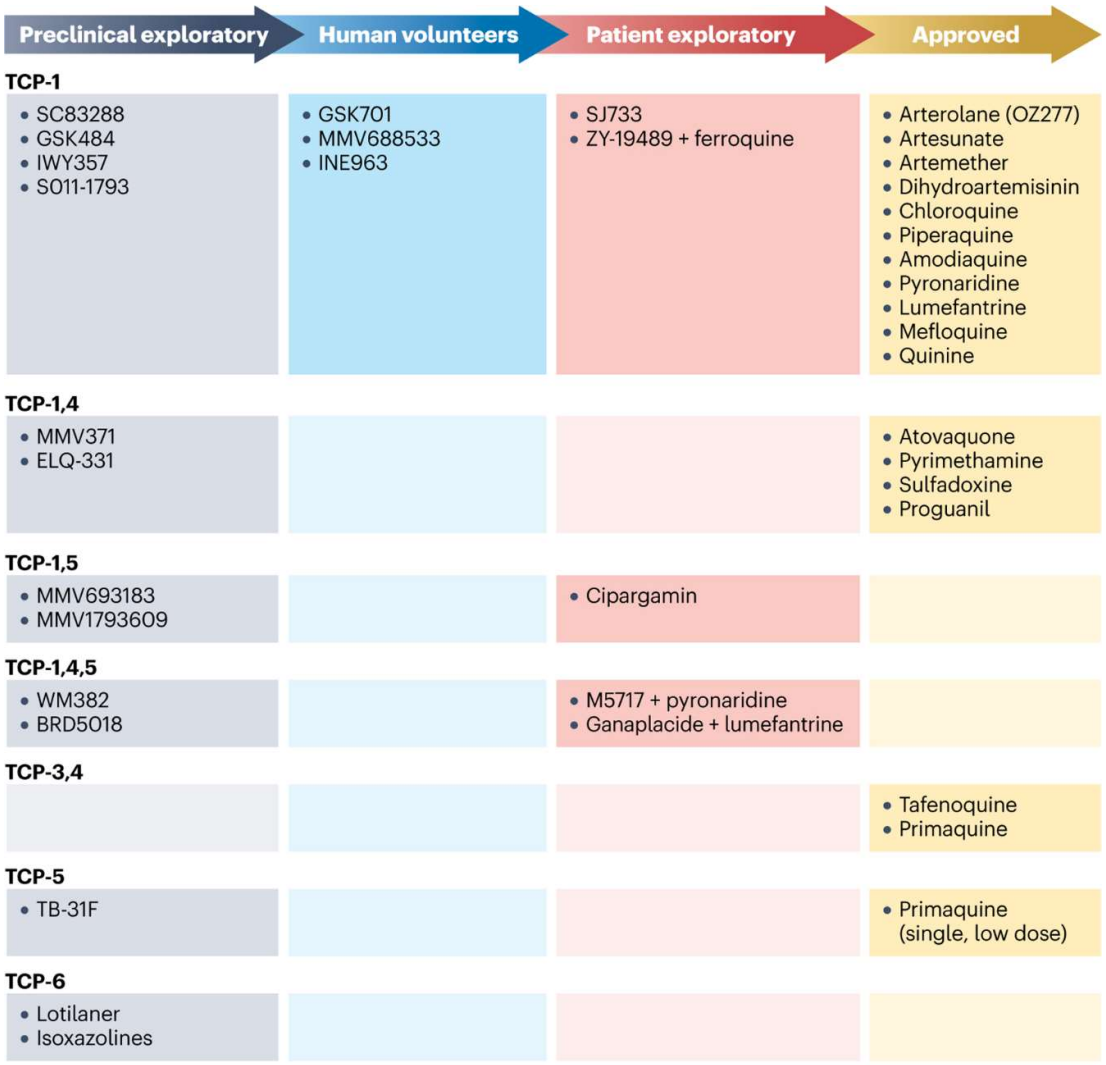

Figure 1.4: MMV's pipeline of antimalarial drugs. MMV-approved and currently used antimalarials, as well as those under development, with their corresponding TCPs representing the stage of disease being targeted. Image is taken from Siqueira-Neto *et al.*, 2023 [43].

1.5. Transmission-blocking antimalarials

At present, the discovery and development of combinations of dual-active antimalarials demonstrating equipotent activity against ABS parasites (TCP-1) and mature gametocytes (TCP-5) is a focus area. There is a fundamental difference in the biology between ABS parasites and gametocytes. ABS parasites are proliferative and undergo a variety of unique morphological changes throughout their development, from the rather quiescent ring stage to the highly metabolically-active trophozoite stage, in which rapid DNA replication occurs, followed by nuclear division in the schizont

stage [44]. Additionally, ABS parasites are associated with fermentative metabolism, owing to elevated metabolic flux through glycolysis and the activation of the Warburg effect [45]. In contrast, DNA replication and nuclear division do not occur in the non-proliferative gametocytes [46], and a shift towards oxidative metabolism is seen [47].

Throughout the ABS proliferation phase of the parasite, drug-resistant strains are inevitably selected for, and once this resistance has arisen in the ABS stage, it is easily transferred to the gametocytes [48, 49]. This enhanced transmissibility is linked to the propensity for some drug-resistant parasites to yield elevated gametocyte numbers following drug-induced stress, as opposed to drug-sensitive ones, consequently leading to increased spread of resistance [50]. As mentioned, gametocyte-specific antimalarials can be combined with compounds targeting the ABS parasites. In this instance, the burden of resistance development can be reduced by blocking transmission and preventing reinfection [47]. Compared to compounds targeting ABS parasites, gametocyte-specific antimalarials are presumed to target unique biological processes because of the different biology associated with ABS proliferation and gametocyte differentiation. In addition to the lower number and non-replicating nature of gametocytes, this makes it highly unlikely that resistance will develop towards transmission-blocking antimalarials [32].

Phenotypic screening of large chemical libraries has contributed significantly to the discovery of novel antimalarials and is, therefore, typically the first step in the drug discovery and development pipeline to identify antimalarial hits [51]. However, a key drawback of phenotypic screening is the lack of knowledge regarding a compound's MoA and drug target [52]. Although information on the specific drug target is not required for registration, it is vital to accelerate antimalarial development. This allows cross-resistance, toxicity and activity to be monitored and facilitates structure-based drug design, optimization, safety evaluation and rational use in drug combinations [36, 51]. More than ever, it is crucial that the next generation of antimalarials includes compounds with unique MoA and high barriers to resistance development [53].

1.5.1. Work leading up to this project

Previous work by Reader *et al.*, 2021, investigated 400 structurally diverse compounds from the MMV Pandemic Response Box (PRB). Parallel *de novo* screening of the PRB was performed against *P. falciparum* ABS parasites, stage IV/V gametocytes and liver stage parasites (*P. berghei*), as well as against gametes, oocysts and as endectocides. Hits were identified against multiple stages of the *Plasmodium* life cycle and specific hits against single stages. These included hits with selectivity (>10-fold) towards late-stage gametocytes with potent transmission-blocking activity [54]. Of these hits, MMV1580843 (from here on referred to as MMV843), was identified as a unique chemotype structurally distinct from any current antimalarial, exhibiting potent transmission-blocking activity (Figure 1.5). This gametocytocidal compound was validated as active against male gametes, which generally have an increased drug sensitivity compared to female gametes [54].

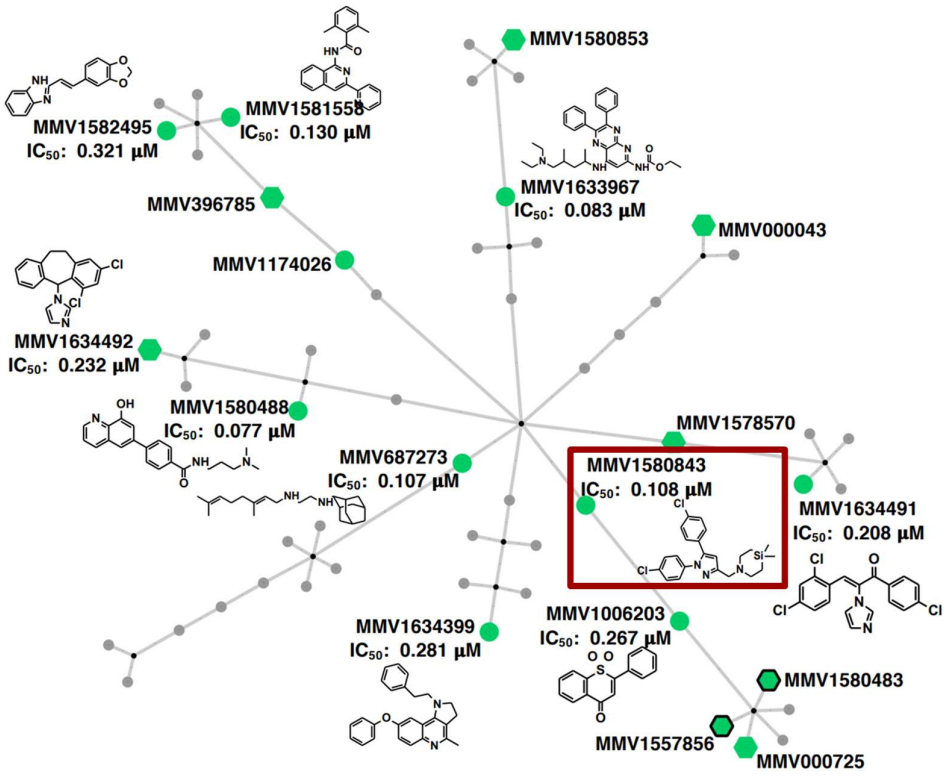

Figure 1.5: Compounds identified as hits from the PRB with gametocyte-selective activity. Structures, compound names and IC_{50} values are indicated for selected compounds. Gametocyte selective compounds are indicated in green. Compounds clustered together have structural similarity. The compound with a red square around it was prioritized in this project. Taken from Reader *et al*., 2021 [54].

MMV843 stems from optimization campaigns of antitubercular drugs, BM212 (Figure 1.6A) and rimonabant (Figure 1.6B). A scaffold-hopping approach revealed notable structural similarities between the anti-obesity agent, rimonabant, and BM212, motivating further investigations into rimonabant and its analogues for antitubercular activity [55]. BM212 is a 1,5-diarylpyrrole derivative, belonging to a class of MmpL3 (mycobacterial membrane protein, large 3) inhibitors [56], with potent activity against both *Mycobacterium tuberculosis* and other non-tuberculosis mycobacteria [57]. BM212 inhibits mycobacterial growth by blocking the transport of mycolic acids, which are required for cell wall synthesis [56]. Rimonabant blocks the cannabinoid receptor-1 (CB1), which is involved in the regulation of food intake, anxiety disorders and mood [58]. Rimonabant has also been shown to directly target MmpL3 [59]. The rimonabant scaffold has the added benefit of crossing the blood-brain barrier, which could be significant in developing antitubercular medications to treat brain *Tuberculosis*. Several rimonabant analogues were generated with varied structural features including silicon incorporation. Of these, the silicon-containing analogue, MMV843 (Figure 1.6C), had the most potent antitubercular activity, attributed to the enhanced cell wall permeability of lipophilic sila compounds [55]. Carbon-silicon (C/Si) bioisosteric replacement into drug discovery and approved drugs is a widely recognized method for adjusting selectivity, physicochemical properties, and drug-like characteristics within pharmacophores. Silicon is considered a suitable alternative to

carbon due to its comparable intrinsic traits, which may result in enhanced pharmacological profiles and improved drug-like attributes [60, 61].

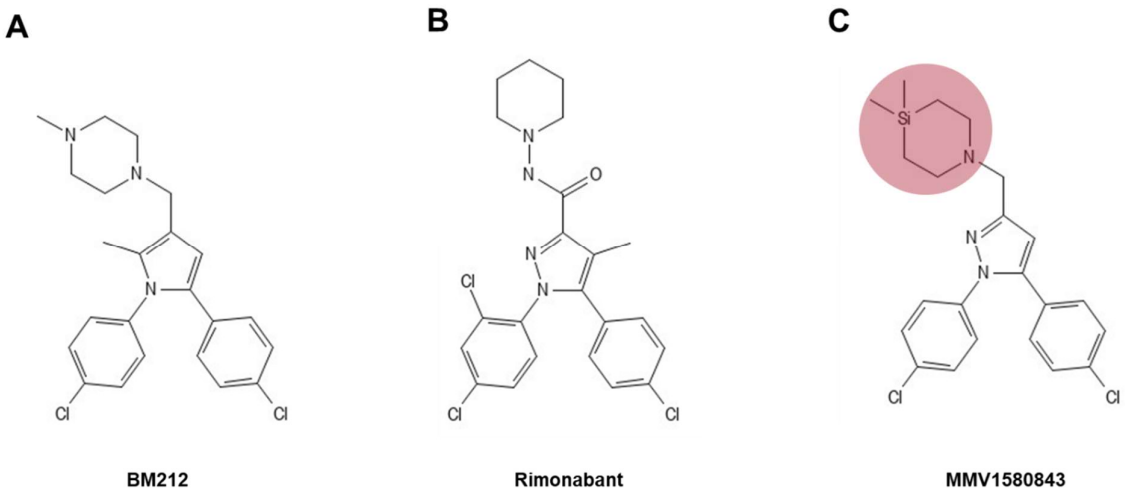

Figure 1.6: Chemical structures of BM212, Rimonabant and MMV843. A. Structure of BM212, an MmpL3 inhibitor. **B.** Rimonabant, CB1 receptor modulator. **C.** MMV843, the silicon analogue of rimonabant. Images adapted from Ramesh *et al*., 2016 [55].

Since MMV843 was shown to have potent transmission-blocking and stage-specific activity towards non-proliferative gametocytes [54], in addition to having a unique silicon-containing structure, a possible novel MoA could be present in *Plasmodium*. This project thus aimed to determine the MoA of MMV843 against *P. falciparum* to facilitate the compound's progression through the drug discovery and development pipeline.

1.6. Strategies to investigate antimalarial drug targets and/or MoA

Novel tool compounds discovered through large phenotypic screening efforts have been used in target identification strategies and/or to describe (at the very least) the MoA of compounds for the past decade [43]. MoA is referred to here as the ability to describe the phenotypic profile that a specific compound elicits on the parasite, whilst target identification refers to the actual protein target to which it is bound.

In vitro evolution), colloquially referred to as resistance selection, and whole-genome analysis (IVIEWGA) has proven effective to discover and identify numerous chemically validated targets, with this compound-dependent approach being the most successful method to date. IVIEWGA involves the selection of resistant parasites that developed drug target mutations following the treatment of proliferative ABS parasites at sublethal concentrations of the compound [62]. Subsequently, precise

locations of the resistance-conferring mutations are identified through whole-genome analysis and comparative genomics between resistant and wild-type parasites. These mutations typically localise either in putative target genes of the compound or in other areas of the genome containing proteins that may confer resistance. Drawbacks to this approach include possible non-specific mutations and general difficulty surrounding the generation of resistant parasites [36, 43]. Additionally, due to the non-proliferative nature of gametocytes, this approach cannot be used to identify the target of gametocyte-specific antimalarials.

Several additional functional genomics methods have been applied to discover antimalarial candidates' MoA and/or drug targets. Metabolomic profiling involves the drug treatment of parasites and subsequent monitoring of fluctuations in parasite metabolites to describe the MoA of a compound. In certain situations, a detectable "fingerprint" is produced due to disruptions in particular metabolic pathways [63-65]. This method is most successful when there is access to metabolic fingerprints of known inhibitors for comparison; however, this is very limited to ABS parasites alone.

Chemical proteomics combines affinity chromatography and mass spectrometry to identify potential targets. Here, a compound of interest is attached to beads to allow the ‘pull-down’ of interacting proteins from the parasite. The disadvantage of this technique is that the target binding of the compound may be compromised after attaching to the bead. Thermal proteomic profiling or cellular thermal-shift assays (CETSA) are alternative strategies that can be employed. The underlying principle of both techniques is that a protein target’s thermal stability is dramatically increased upon compound binding; however, this increase in thermal stability does not confirm whether that protein is the true or exclusive target of the compound. Finally, chemoinformatic tools or computer-aided drug discovery may be used to investigate possible targets by performing compound similarity searches utilizing known antimalarials with validated drug targets or through molecular docking approaches. Although *in silico* approaches provide interactions between a compound and a potential target, extensive follow-up validation is critical [36, 43].

Current conventional target identification and MoA studies centre on the proliferative ABS parasites due to technical and biological constraints, including challenges related to their lower abundance, purification, non-proliferative nature, and limitations in culturing conditions, when working with gametocytes. Investigating gametocyte-specific antimalarial targets is more challenging since transmission-related processes implicated in the *P. falciparum* life cycle are less understood. Therefore, since most conventional target identification strategies are limited to ABS parasites, finding novel approaches to establish the targets of compounds specific to non-proliferative gametocytes is crucial.

1.7. Therapeutically attractive organelles in *P. falciparum*

Mitochondria play a crucial role in cellular energy production and various metabolic processes in numerous organisms, including *P. falciparum*. Apart from ubiquinone recycling in pyrimidine biosynthesis [66], *P. falciparum* ABS parasites are not dependent on oxidative phosphorylation (OXPHOS) and thus have a considerably lower number of OXPHOS complexes compared to gametocytes. By contrast, *P. falciparum* gametocytes depend on OXPHOS for successful development and colonization within the mosquito vector, with multiple additional mitochondrial functions, including active respiration, and playing a critical role [67-70]. Interestingly, in gametocytes, respiratory chain complex components and associated metabolic pathways are as much as forty times more widespread, accompanied by a substantial decrease in glycolytic enzymes. The significance of mitochondria in cellular energy production and metabolic processes underscores their pivotal role in the intricate life cycle of *Plasmodium* and thus presents an attractive target in drug discovery.

In various organisms, the endoplasmic reticulum (ER) is a multifunctional organelle involved in the synthesis, folding and secretion of proteins, lipid metabolism, and calcium storage, making it crucial for various cellular processes. Previous studies investigating ER morphology in *P. falciparum* ABS stage parasites stated that the ER resembles a ring encircling the nucleus that extends into the cytoplasm and, in late stages, becomes significantly branched [71, 72]. *Plasmodium* has a relatively ordinary collection of secretory organelles, including an ER and a single Golgi apparatus, in addition to its specialized organelles [73]. Their morphology and biosynthesis have only been partially described thus far, and mainly in the context of *Plasmodium* ABS parasites. Gametocytes (stage I-III) produce a large number of ribosomes and ER. This is consistent with the young parasite's active synthesis of RNA and proteins [74]. Gametocytes take on a falciform, or crescent, shape due to developing a microtubule network tethered to a cisternal inner membrane complex (IMC) [75]. The ER and the IMC membranes were previously found to be closely associated by super-resolution imaging [76], deeming the ER important in gametocyte development. In another study, ER accumulations were reported in both ABS parasites and in gametocytes. These ER accumulations have been described as functional subdivisions of the ER, characterized as large, intricate, and dense ER tubule networks, most likely produced due to increased parasite demands, which may be associated with ER stress. *Plasmodium* parasites have a substantially decreased unfolded protein response machinery for responding to ER stress compared to higher eukaryotes. Consequently, applying ER stress may be exploited to disrupt parasite development [71].

By employing a mechanism of invagination, *Plasmodium* enters the RBCs of the human host, creating a parasitophorous vacuolar membrane (PVM) that encloses the parasite, which is then modified by the aid of its secretory organelles. The PVM functions by isolating the parasite and acting as a protective barrier, inhibiting the destruction of the parasite by lysosomal machinery in the host cells [77]. The most researched PVM protein exclusive to gametocytes is Pfs16 [78, 79], which is an

early indicator of sexual commitment and is considered crucial for preserving the stability and integrity of the PVM [80]. The PVM and, in most cases, the IMC, are closely associated with the gametocyte plasma membrane [4]. *Plasmodium* depends on lipids for membrane biosynthesis, haemoglobin breakdown, protein trafficking, and signalling. However, it should be noted that the lipid content of gametocytes, as compared to the ABS parasites, differs drastically [81]. Specifically, an enrichment of sphingolipids implicated in ceramide metabolism is seen for all stages of gametocytes and plays a crucial role in maturation. In contrast, a decline in glycerolipid and phospholipid levels is observed [4, 81, 82]. Additionally, numerous lipids diminished in early gametocytes and trophozoites are restored in late-stage gametocytes, including mediators of membrane fluidity. In the mosquito vector, where the availability of certain lipid species is restricted, the strikingly abundant neutral lipids in mature gametocytes may function as a considerable energy store to support the increased phospholipid and protein biosynthesis needed during gametogenesis and early zygote development [82]. The phosphatidylcholine synthesis pathway is vital for gametocytogenesis and mosquito transmission, and new antimalarial compounds have been discovered that specifically target lipid synthesis-related enzymes as well as signaling lipids and membranes [83-85].

The food (digestive) vacuole (FV) is an acidic lysosome-like organelle shown to be present in both stage I-V *P. falciparum* gametocytes [4, 45] and ABS parasites [86]. Haemoglobin catabolism and heme detoxification are the FV's primary functions; however, the roles it plays in ion homeostasis and lipid utilization are still poorly understood [86]. Within the malaria parasite, vesicles containing host-derived haemoglobin are transported to the FV, where phospholipases break down the surrounding membrane. Subsequently, a cascade of proteases digest the haemoglobin resulting in the production of a significant amount of haem [87], a toxic molecule which may prevent enzymic processes, disrupt membranes and commence oxidative damage [88, 89]. To counteract this, a characteristic insoluble haemozoin crystal is formed within the FV and thus detoxification is achieved [90, 91]. By keeping the RBCs' osmotic stability intact and supplying the parasite with the amino acids needed for its protein synthesis, this proteolysis prevents the host cell's premature hemolysis [92, 93]. Given the unique and vital processes that take place in this organelle, the FV of the malaria parasite is an established target for several antimalarials, and thus houses transporters associated with drug resistance [94]. The very susceptible FV housed by *Plasmodium* parasites can be exploited in chemotherapeutics, owing to the permanent risk of oxidative damage resulting from a surplus of haem [86, 95, 96].

The essential roles the mitochondria, ER, parasite membrane and FV play in the parasites' cellular functions present an opportunity to explore and understand a compound’s MoA, as potential morphological differences between untreated and treated parasites may be indicative of specific drug effects.

1.8. Morphological and biochemical profiling of drug action

Morphological profiling has successfully classified drug target pathways based on how an organism responds to drug treatment. In fact, this technique has been used to elucidate the MoA [97-101], gene interactions [102, 103], describe cellular heterogeneity [104] and identify targets [102, 105] of investigative compounds in various organisms. This has been particularly successful in the antibacterial field, where image automation has resulted in high-throughput systems able to detect changes in morphological features in a cell [106]. In this way, morphological fingerprints can be compiled, where specific small molecule classes produce similar phenotypes. The application of machine learning for image recognition, classification, and prediction provides access to a vast underexplored field of data that could contribute to accurately describing a drug candidate's MoA [107].

Complex morphological profiling systems, such as the now coined 'Cell Painting' technique, aim to probe several cellular architectures, organelles or biochemical functions with fluorescent dyes to identify biologically relevant characteristics associated with a particular drug treatment [108]. This technique exploits the ability of compounds to affect the essential organelles (as discussed above) and this can be traced by fluorescent dyes to simultaneously evaluate the nucleus, mitochondria, ER, cytoskeleton, RNA and Golgi apparatus (Figure 1.7). Whilst this high-content data is inherently qualitative, multiplexing of several fluorescent dyes can now also be quantified and statistically validated [108].

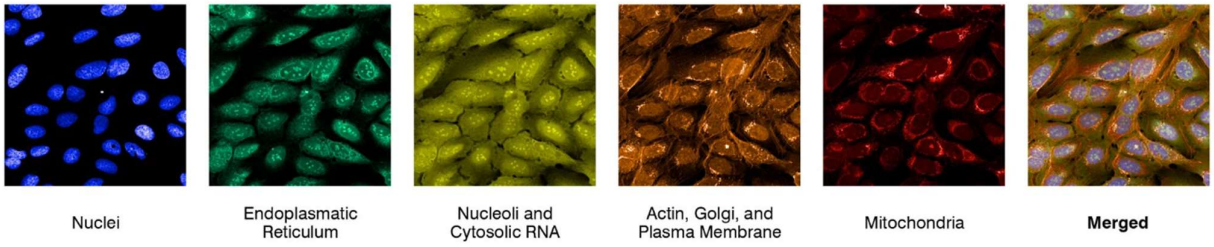

Figure 1.7: Eight cellular organelles visualized with five fluorescent dyes. Cells are stained with a set of fluorescent dyes that bind to specific cellular organelles. The dyes used in Cell Painting are selected to provide a comprehensive view of cellular morphology and organization. Image taken from Charles River Laboratories website [109].

The Cell Painting technique can be used to investigate a variety of different cell types. To determine a compound's MoA, this technique can interrogate and analyze morphological changes or compare staining patterns, pre- and post-treatment, to those of a compound with an established target (Figure 1.8). The Cell Painting technique has been extensively used to characterize the MoA of drugs in the cancer field. For instance, a study at the Broad Institute of MIT and Harvard utilized cell painting to identify the potential MoA of novel compounds and develop predictive models that could anticipate a compound's effects on specific cellular components [110]. Another study used cell painting to screen compounds for drug repurposing opportunities and new therapeutic targets in oesophageal

cancer [111]. This study generated a phenotypic fingerprint for every cell, following chemical or genetic perturbation, to identify chemical starting points and novel targets and guide MoA studies. Additionally, another study found that a significant proportion of known bioactive compounds yielded significant changes in image-based profiles, and machine learning could be used to improve the analysis of cell painting data [112].

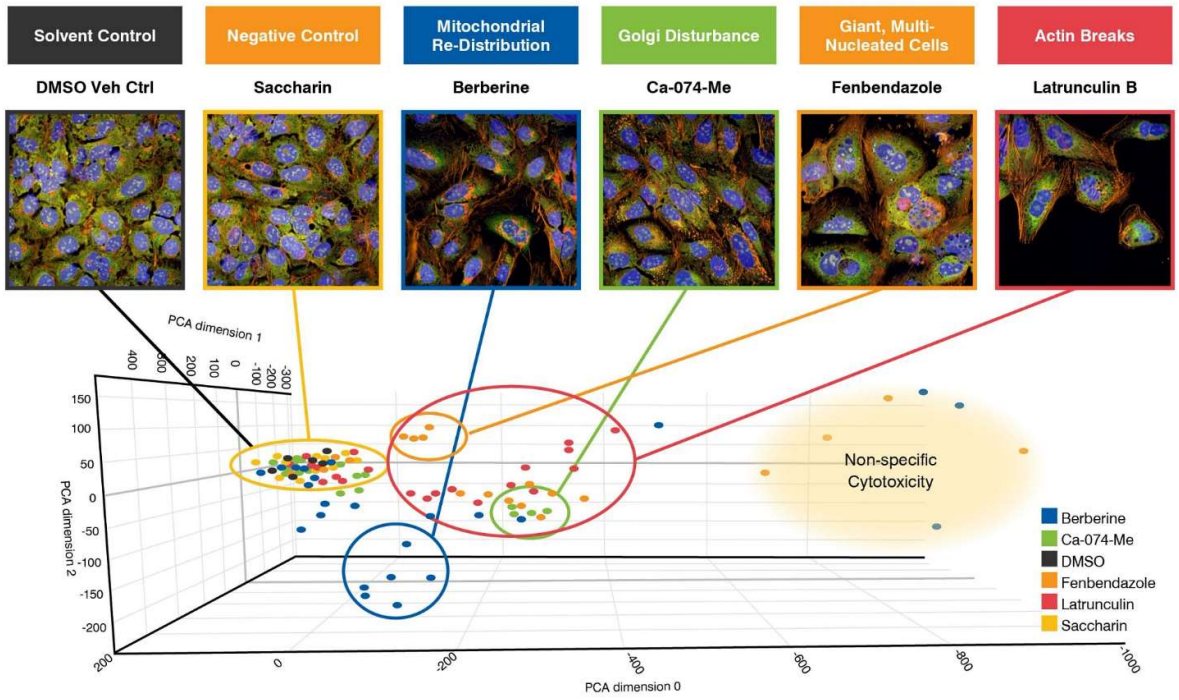

Figure 1.8: Cell Painting reference compounds, with established targets, to investigate MoA of novel compounds. A 48 h treatment with each reference compound exhibits unique morphological phenotypes. Principal component analysis (PCA) plots confirm unique phenotypic effects and additionally, at higher concentrations, demonstrate non-specific cytotoxicity. Image taken from Charles River Laboratories website [109].

Although Cell Painting has successfully been utilized in numerous cells, it has not been applied to *Plasmodium* [108]. Given the complications surrounding the investigation of drug MoA in gametocytes and the unique morphology and biology associated with this stage, the principle of this technique can be used as a powerful tool for target identification. There is a lot of potential for this in antimalarial drug discovery and, therefore, this study aimed to take the principle of Cell Painting through to *P. falciparum* gametocytes to explore the MoA of the gametocyte-specific drug, MMV843. However, because this complex principle of combining different dyes together in a single staining step has not been explored in *Plasmodium*, this project opted for individual staining of organelles to ensure useable data was obtained.

2. Aim

This project aimed to determine the organelles implicated in the MoA of MMV843 against late-stage gametocytes using complementary biochemical approaches.

2.1. Hypothesis

Fluorescent indicators and cell-based analyses of biochemical pathways can reveal differences between MMV843-treated and untreated parasites to indicate its MoA.

2.2. Objectives:

I. Chemoinformatic target predictions of MMV843.
II. Determining the effect of MMV843 against late-stage gametocytes.
III. Evaluating the involvement of various biochemical processes in the MoA of MMV843.
IV. Determining cross-reactivity of MMV843 to known antimalarials with validated MoA.

3. Methods and Materials

3.1. Cheminformatics

3.1.1. Target prediction

The parent compounds of MMV843 (BM212 and rimonabant) have been shown to directly target MmpL3 in *M. tuberculosis* [59]. The *M. tuberculosis* amino acid sequence of MmpL3 (Uniprot ID: P9WJV5) was obtained from UniProt (https://www.uniprot.org/). This sequence was used to search for homologues in *P. falciparum* using the BlastP tool in PlasmoDB (https://plasmodb.org/) based on sequence similarity and sequence identity.

Similarity Ensemble Approach (SEA) (https://sea.bkslab.org/) was used to search for additional novel targets of MMV843 in any organism. Proteins are compared by leveraging the set-wise chemical similarity between their ligands and can thus create cross-target similarity maps and search extensive compound databases with ease [113]. The Simplified Molecular Input Line Entry System (SMILES) string for MMV843 was submitted to SEA under standard parameters. A list of possible targets was obtained with associated P-values, indicating the likelihood of target specificity. The top two targets with the best P-values were used in searches for *P. falciparum* orthologues. The amino acid sequences of these top targets obtained from UniProt were used to search for homologues in *P. falciparum* using the BlastP tool in PlasmoDB.

3.1.2. Target modelling

The *P. falciparum* protein structures were obtained from AlphaFold, which uses machine learning to solve protein structures by leveraging chemical and physical properties [114, 115]. All structures were imported into Schrödinger Maestro (2022-4). Structures were prepared using the Protein Preparation Wizard under default parameters to add in hydrogens, remove steric clashes and energy minimise the structures. Missing side chains were filled in using the Prime module of Schrödinger.

3.1.3. Docking for virtual screening of compounds

Potential binding sites of MMV843 and BM212 were identified and ranked according to ligand-binding amenability using SiteMap based on binding pocket size and solvent exposure. The parent compound BM212 was used as a comparative control since MMV843 has greater structural similarity to BM212 (tanimoto coefficient: 0.42) compared to rimonabant (tanimoto coefficient: 0.25). Binding sites were selected for docking, informed by InterPro annotation, where binding pockets containing residues annotated as constituting the active site were used. Ligands were prepared and desalted using LigPrep for energy minimisation and identification of different protonation and tautomeric states at a pH range of 7.0 ± 2.0. Receptor grids were created centred on the sites identified using SiteMap. A ligand diameter midpoint box size of 10-20 Å in every dimension was used. Docking was performed using extra precision mode and binding poses were rank ordered according to XP GScore [116].

3.2. *In vitro P. falciparum* parasite cultivation

3.2.1. Ethical clearance statement

All *in vitro* experiments involving the use of *P. falciparum* parasites were conducted in a biosafety level 2 (BSL2) certified malaria culture facility at the University of Pretoria in the Malaria Parasite Molecular Laboratory (M^2PL) (registration number: 39.2/University of Pretoria-19/160). This study was covered by an umbrella ethical clearance for the SARChI program provided to Prof L Birkholtz (reference: 180000094) by the Faculty of Natural and Agricultural Science. Clearance for the use of human erythrocytes was approved by the Faculty of Health Science Ethics Committee (ethics approval no: NAS298/2022).

3.2.2. Culturing of asexual parasites

Asexual *P. falciparum* parasites from the drug-sensitive NF54 clonal strain were cultivated under sterile conditions in BSL2 biosafety cabinets in human RBCs (5 % haematocrit, various blood types) in complete culture media (RPMI-1640 cell culture medium (Sigma-Aldrich, USA) supplemented with 25 mM HEPES (pH 7.5, Sigma-Aldrich, USA), 23.81 mM sodium bicarbonate (Sigma-Aldrich, USA), 0.024 mg/mL gentamicin (HyClone, USA), 0.2 % (w/v) D-glucose (Merck, Germany), 0.2 mM hypoxanthine (Sigma-Aldrich, USA) and 5 g/L AlbuMAX II (Life Technologies, USA, as a human serum alternative) [117, 118]). Parasite cultures were incubated at 37 °C with continuous agitation (60 rpm) in an orbital shaker-incubator [119] and under hypoxic conditions (5 % CO_2, 5 % O_2 and 90 % N_2) (Afrox, South Africa) to mimic the natural environment experienced by the parasite [120]. Parasitaemia (number of iRBCs in 1000 RBCs) was evaluated daily using RapiDiff stain on methanol-fixed thin smears of parasite samples. The stained smears were visualized with oil immersion at 1000x magnification, employing a YS2-H Nikon microscope (Nikon, Japan) to examine parasite morphology and assess parasitemia.

3.2.3. Synchronisation of asexual parasites

Ring-stage ABS parasites were treated with 5 % (w/v) D-sorbitol, to synchronize parasites by inducing osmotic lysis of schizont- and trophozoite-infected RBCs, killing these stages [121, 122]. After 15 min of incubation at 37 °C in pre-warmed 5 % (w/v) D-sorbitol, the parasite cultures were centrifuged for 5 min at 1800 x*g* (Heraeus Megafuge 40 centrifuge, Thermo Scientific, USA), and lysed parasite debris and excess sorbitol removed by washing twice with incomplete culture media (complete culture media as described above lacking AlbuMAX II). Following this, the parasite pellet was resuspended in complete culture media to create a 5 % haematocrit culture, which was thereafter maintained as described in section 3.2.2.

3.2.4. Induction of gametocytogenesis

Gametocytogenesis was induced from the synchronous ring-stage (>90 %) *P. falciparum* NF54 ABS parasites by decreasing haematocrit and through nutrient starvation to mimic the natural stress response experienced by the parasite [123]. The parasitaemia of the ABS parasite cultures was adjusted to 0.5 % in 6 % haematocrit, and the culture was transferred to complete culture medium without glucose supplementation [121]. The cultures were maintained, without shaking, at 37 ºC under hypoxic conditions. After 72 h, gametocytogenesis was induced by decreasing haematocrit to 4 % and incubating as previously described. From day 3 post-induction, the remaining ABS parasites were eliminated by continuous treatment with 50 mM *N*-acetyl glucosamine (NAG) in complete culture medium containing glucose, to ensure viability of gametocytes was maintained [124]. Gametocytes were observed daily (determining gametocytaemia as the number of iRBCs by counting 1000 individual RBCs) using RapiDiff stain on methanol-fixed thin smears of parasite samples and visualized with oil immersion at 1000x magnification with a YS2-H Nikon light microscope (Nikon, Japan).

3.3. Kinetic/rate of action study against late-stage gametocytes

P. falciparum NF54 parasites were cultivated *in vitro* as described in section 3.2. MMV843 was initially dissolved in DMSO to a concentration of 10 mM. A volume of 150 µL per well of *P. falciparum* late-stage gametocytes (4 % haematocrit, ≥1.8 % gametocytaemia) was added to a 96-well plate already containing 50 µL of complete RPMI culture medium treated with either 468 nM or 2 340 nM of MMV843 to give a final concentration of 117 nM (1x IC_{50}) or 585 nM (5x IC_{50}) in a final volume of 200 µL/well. The IC_{50} value is the concentration of drug required for 50 % inhibition of gametocyte viability. The IC_{50} value of MMV843 (117 nM) used was determined against late-stage gametocytes on the PrestoBlue assay by Reader *et al.* [54]. The negative control for this assay was 50 µL of complete RPMI culture medium free from drug treatment to ensure any decrease in gametocyte viability was due to drug treatment and not general culture death. Additionally, a positive control for inhibition of 50 µL of methylene blue at 1 µM was included to confirm death at each time point. The 96-well plate was then incubated under hypoxic conditions within a stationary incubator at 37 °C. Gametocytes were exposed to drug pressure for 6, 12, 24 or 48 h. Subsequently, excess media was removed from the drug-treated and control wells, at each stipulated time point, and the remaining pellet was used to make methanol-fixed, thin smears stained with RapiDiff stain. In addition, a RapiDiff stained, methanol-fixed thin smear was made using the untreated, positive control at 0 h to establish the starting gametocytaemia in each well. Following this, gametocyte viability (obtained by counting 100 individual gametocytes and visually determining them as dead or alive) was assessed and gametocytaemia was determined at each time point for the control and drug-treated gametocytes using a YS2-H Nikon light microscope (oil immersion at 1000x magnification; Nikon, Japan). The above was performed for three independent biological replicates (n = 3).

3.4. Confocal microscopy of live late-stage gametocytes

To evaluate the involvement of various biochemical processes in the mode of action of MMV843, organelle-specific fluorescent dyes were used to visualize and, therefore, compare MMV843-treated gametocytes and untreated gametocytes. MMV390048-treated gametocytes (from here on referred to as MMV048) were used as a positive drug control. Apart from liver hypnozoites, MMV048 is active against all *Plasmodium* life cycle stages having phosphatidylinositol 4-kinase (PI4K) as the proven target [125].

3.4.1. Fluorescent dyes used for organelle staining

JC-1 is a lipophilic, cationic probe (naturally producing green fluorescence) that can detect mitochondrial membrane potential in drug-treated and untreated parasites. JC-1 accumulates in mitochondria, due to the electronegative environment within the mitochondria, forming complexes termed J aggregates which result in red fluorescence. When the mitochondrial membrane is depolarized, and thus has a low membrane potential, possibly due to increased membrane permeability resulting from drug treatment, JC-1 remains in its monomeric form and thus retains its original green fluorescence [126, 127]. ER-Tracker Red (BODIPY TR Glibenclamide) is a highly selective and photostable ER probe which emits red fluorescence [128]. ATP-sensitive K^+ channels, prominent on the ER, have sulphonylurea receptors that glibenclamide (glyburide) binds to with selectivity [71, 129]. BODIPY-TR-ceramide is a lipid membrane probe which emits red fluorescence. Since D-*erythro*-sphingosine is used to make BODIPY-TR-ceramide, it shares the same stereochemical structure as naturally occurring, physiologically active sphingolipids. This probe allows for visualising membrane domains, including the parasite plasma membrane, the PVM and the food vacuole membrane [130-132]. LysoTracker Deep Red is a pH-dependent red fluorescent dye which stains acidic organelles, including the lysosome-like FV of the parasite [94, 128, 133]. In its neutrally charged state, LysoTracker probes, which comprise a hydrophobic fluorophore attached to a weak base, can diffuse readily across intact plasma membranes of live cells. However, upon entry into an acidic organelle, the weakly basic moiety becomes protonated, and the probe is subsequently sequestrated within the acidic environment [134].

3.4.2. Sample treatment and preparation

In a 1.5 mL Eppendorf tube, 250 µL of late-stage gametocytes were treated with compound at the following concentrations and time periods: 1x IC_{90} (801.4 nM) of MMV843 for 6 h; 2x IC_{50} (234 nM) of MMV843 for 24h and 2x IC_{50} (280.6 nM) of MMV048 for 24h with untreated gametocytes as an uncompromised control. The above treated and untreated parasites were incubated at 37 °C under hypoxic conditions within a stationary incubator for each stipulated time period. Following the compound incubation periods, the Eppendorf tubes were transferred to a heating block (37 °C) and co-stained with 1 µg/mL Hoechst 33342 for 10 min (Invitrogen by Thermo Scientific, USA) and one of the organelle-specific dyes detailed in Table 3.1 (all dyes were obtained from Invitrogen by Thermo Scientific, USA). Hoechst 33342 DNA dye was included in each sample to confirm the visualization

of parasites. Hoechst 33342 is a blue fluorescent, DNA-specific dye which attaches to the minor groove of double-stranded DNA, showing a preference for regions rich in adenine and thymine (AT), which are notably abundant in the *Plasmodium* genome, constituting over 80% in the majority of species [75, 128].

Table 3.1: Organelle-specific fluorescent dyes used to visualize *P. falciparum* gametocytes.

Stain/dye	Concentration	Incubation time	Organelle stained
JC-1	0.5 µM	30 min	Mitochondria
LysoTracker Deep Red	0.2 µM	30 min	Acidic organelles
ER-Tracker Red (BODIPY TR Glibenclamide)	0.5 µM	30 min	Endoplasmic reticulum (ER)
BODIPY-TR-ceramide	0.7 µM	Overnight (18-24 h)	Membrane

Once staining was complete, the parasite samples were centrifuged for 30 s at 5 000 x*g* (SL 8R, Thermo Scientific, USA) and the supernatant was removed, being careful to not disrupt the pellet. Finally, to wash out excess stain, the pellet was carefully resuspended in 250 µL of pre-warmed sterile filtered Ringer's solution (pH 7.4; 25 mM HEPES; 122.5 mM NaCl; 1 mM NaH_2PO_4; 5.4 mM KCl; 11 mM D-glucose; 1.2 mM $CaCl_2$; 0.8 mM $MgCl_2$), centrifuged as above and the supernatant was removed (again being careful to not disrupt the pellet) and replaced with fresh Ringer's solution. This washing step was repeated 2-3 times. After the final wash, the pellet was again carefully resuspended in fresh Ringer's solution and kept at 37 °C until imaging.

3.4.3. Live-cell confocal imaging

Live confocal analysis was conducted at the Laboratory for Microscopy and Microanalysis unit at the University of Pretoria. A volume of 8 µL of sample was transferred onto the middle of a clean glass microscope slide (Lasec, South Africa) and a glass coverslip (thickness no.1 (0.13 – 0.16 mm)) (Lasec, South Africa) was placed over the sample and secured by sealing the edges with nail polish. All confocal microscopy imaging was performed using a Zeiss Confocal Laser Scanning Microscope 880 Elyra, AxioObserver with Airyscan technology (Carl Zeiss, Germany). An alpha Plan-Apochromat 100x/1.46 oil DIC M27 Elyra objective was used, and images were obtained on a single plane. Table 3.2 details the excitation max, emission max, laser wavelength and detection range used for each corresponding stain. Images were then analysed and processed as AiryScan images using ZEN 3.6 (Blue edition) imaging software (Carl Zeiss, Germany).

Fluorescent intensity of images, obtained using the same acquisition settings throughout, was quantified using the Fiji distribution of ImageJ (ver. 1.54f). Images were pre-processed by applying a Gaussian blur filter of sigma 2 to the red channel of each image (corresponding to LysoTracker

Deep Red, ER-Tracker Red, JC-1 aggregates) and the green channel (JC-1 monomers) to smooth out image noise, thereby enabling greater cell segmentation accuracy. Each image was then thresholded and the integrated density of signal for each gametocyte measured. Column scatter graphs were generated using GraphPad Prism 8.0 software.

Table 3.2: Excitation max, emission max, laser wavelength and detection range used for each corresponding stain.

Stain	$\lambda_{ex}/\lambda_{em}$ (nm)	Laser wavelength (nm)	Detection range (nm)
Hoechst 33342	361/486	405	415-490
JC-1 monomers (Green)	514/529	514	507-562
JC-1 aggregates (Red)	514/590	514	575-612
ER Tracker Red	587/615	561	582-728
LysoTracker Deep Red	647/668	633	640-750
BODIPY-TR-Ceramide	589/617	561	579-640

3.5. SYBR Green I based asexual proliferation assay

The SYBR Green I assay was used as it is a simple fluorescence-based technique which is rapid, inexpensive, can be performed in one step and is very sensitive. This assay was conducted to determine the IC_{50} value of CL268 and four antimalarials or in-development candidates with validated drug targets (Table 3.3). The IC_{50} values obtained through this assay were used to perform IC_{50} shifts to investigate potential cross-reactivity with CL268. CL268 is a derivative of MMV843 and since MMV843 has extremely poor asexual activity, CL268 was used as a proxy for MMV843. The structure of CL268 only differs from that of MMV843 by a trifluoromethyl group in place of the chlorine group (Figure 3.1). Furthermore, CL268 has better asexual activity while gametocyte activity is retained. The target of CL268 is unknown but the compound is assumed to have a similar target as its parent compound, MMV843.

Table 3.3: Antimalarials and in-development candidates with validated drug targets in *Plasmodium*, used in this project.

Known antimalarial	Validated drug target
Atovaquone	Cytochrome bc1 (Q_0)
KAF156 (Ganaplacide)	Protein Secretory Pathway
P218	DNA Replication/Transcription
MMV390048	*Pf*PI4K

This assay uses SYBR Green I dye, which is a DNA-intercalating dye, to determine parasite proliferation. The dye has a noticeable affinity for DNA, as well as marked fluorescence enhancement when the SYBR Green I dye interacts with the *Plasmodium* DNA, making the detection of nucleic acid extremely sensitive [135]. Human RBCs do not contain DNA, whereas infected RBCs contain the parasites' DNA, therefore, since SYBR Green I dye shows enhanced fluorescence upon intercalation with DNA, this assay is advantageous when it comes to detecting parasite proliferation [136].

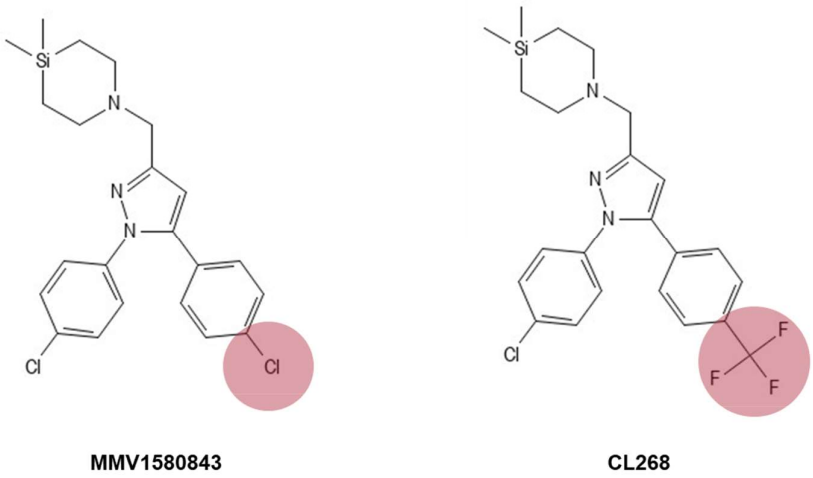

Figure 3.1: Chemical structures of MMV843 and CL268. The structure of MMV843 differs from that of CL268 by replacing a chlorine group with a trifluoromethyl group. Changes are highlighted in red on the structures.

CL268 and the four antimalarials were initially dissolved in DMSO to a concentration of 10 mM. In sterile 96-well plates, a 2-fold serial dilution was set up for each compound at starting concentrations of 16 µM (CL268); 40 nM (atovaquone); 96 nM (KAF156); 800 nM (MMV048) and 20 nM (P218). The controls for this assay included 50 µL chloroquine (1 µM, positive drug control) and 50 µL of complete RPMI culture medium (negative drug control). Chloroquine is a well-established antimalarial and is used as a positive, treated control as it results in high parasite death. Complete culture medium was used as a negative, untreated proliferation control to ensure parasites proliferate without drug treatment. Synchronised ring-stage asexual parasites (50 µL, 1 % parasitaemia and 1 % haematocrit) were added to the drug-containing and control wells to give a final volume of 100 µL/well. The 96-well plates were incubated under hypoxic conditions within a stationary incubator for 96 h at 37 °C. Subsequently, each well was resuspended and 100 µL of SYBR Green I lysis buffer (0.2 µL/mL of 10 000 X SYBR Green I (Invitrogen, USA); 20 mM Tris, pH 7.5; 5 mM EDTA; 0.008% (w/v) saponin; 0.08% (v/v) Triton X-100) was added to the 96-well plates. DNA levels were then quantified, based on the DNA binding properties of SYBR Green I dye, by measuring fluorescence to indicate the effects of the compounds on parasite proliferation [137]. Fluorescence was measured,

with excitation at 485 nm and emission at 538 nm, using the Fluoroskan Ascent FL microplate fluorometer (Thermo Scientific, USA). To determine parasite proliferation, the resulting data were represented as percentage untreated control after subtracting the background (chloroquine-treated control). Dose-response curves were generated using GraphPad Prism 8.0 software with the standard error-of-the-mean (S.E.) indicated. Each compound was tested in technical triplicates for three independent biological replicates (n = 3).

3.6. IC_{50} shift assays

To further explore the possible targets of MMV843, cross-reactivity of CL268 (the proxy for MMV843) to known antimalarials with validated drug targets was investigated to test for the possible potentiation of drug effect. The parasites were treated with sublethal concentrations of the four compounds with known drug targets (Table 3.3). An increase in sensitivity of the parasites to CL268 seen after treatment in the presence of the known antimalarial suggests that the parasites exposed to CL268 are highly sensitive to alterations in that specific drug target [138] and will present with a shift in IC_{50}.

Ring-stage asexual parasites (1 % parasitaemia, 1 % haematocrit) were cultured and synchronised as described in sections 3.2.2 and 3.2.3. SYBR Green I assays were performed, as described above in section 3.5., with slight changes in procedure. Here two compounds were used instead of one, including CL268 and one of the four antimalarials with known drug targets per plate set-up. In sterile 96-well plates, a 2-fold serial dilution was set up for CL268, at a starting concentration of 8 µM, to achieve an 8-point curve. The controls for this assay included a positive drug control (50 µL of chloroquine at 1 µM) and two negative controls (50 µL of complete RPMI culture medium). Half of the parasite suspension was left untreated and added to the top three rows of 2-fold serially diluted CL268, the chloroquine control, and one of the negative controls to give a final volume of 100 µL/well. The remainder of the parasite suspension was divided equally into four parts and treated with each of the four antimalarials at the determined IC_{50}. Following this, the drug-treated parasite suspensions were added to the bottom three rows of 2-fold serially diluted CL268 and the other negative control wells, respectively, giving a final volume of 100 µL/well. Parasites treated with CL268 alone were used to determine the fold change in IC_{50} with respect to those treated with both CL268 and each of the four individual antimalarials. The 96-well plates were incubated under hypoxic conditions within a stationary incubator for 96 h at 37 °C. Fluorescence was again measured as described in section 3.5. The resulting data was normalised to the negative controls (untreated and IC_{50} drug-treated suspensions, respectively) after subtracting the background (chloroquine-treated control). Dose-response curves were generated using GraphPad Prism 8.0 software with the standard error-of-the-mean (S.E.) indicated. Each compound was tested in technical triplicates for three independent biological replicates (n = 3).

4. Results

4.1. Cheminformatics

Given the absence of a confirmed target of MM843 in any organism, including *Plasmodium*, potential targets were investigated through *in silico* analysis. Since the parent compounds of MMV843 (BM212 and rimonabant) have been shown to directly target MmpL3 in *M. tuberculosis* [56, 59], homologues of MmpL3 in *P. falciparum* were first searched for using the BlastP tool in PlasmoDB. No direct homologues to MmpL3 were found since only one protein hit was indicated, namely glucose-6-phosphate isomerase (PF3D7_1436000), with a poor Expect value (E) of 4.0. The Expect value (E) is a statistical parameter representing the probability that a sequence similarity match between database and query sequences occurred by random chance. An E-value is considered significant if the value given is ≤ 10^{-3} [139]. Although there were no direct homologues to MmpL3 in *P. falciparum*, MmpL3 is part of the resistance nodulation-division (RND)-superfamily, of which the *P. falciparum* Niemann-Pick type C-related protein 1 (a parasite plasma membrane lipid transporter, accession code: Q8I266) is a member. In fact, this protein is a druggable target required for maintaining the appropriate parasite membrane lipid composition and thus homeostasis [140]. MMV843 was docked using Schrödinger Maestro (2022-4) into a model that was generated of the *P. falciparum* Niemann-Pick type C-related protein 1 structure with AlphaFold(Figure 4.1). Additionally, the parent compound BM212 was similarly docked into this structure as a comparative control. Three different tautomeric forms for BM212 are present at physiological pH, whereas there was only one tautomeric form for MMV843 (Figure 4.1).

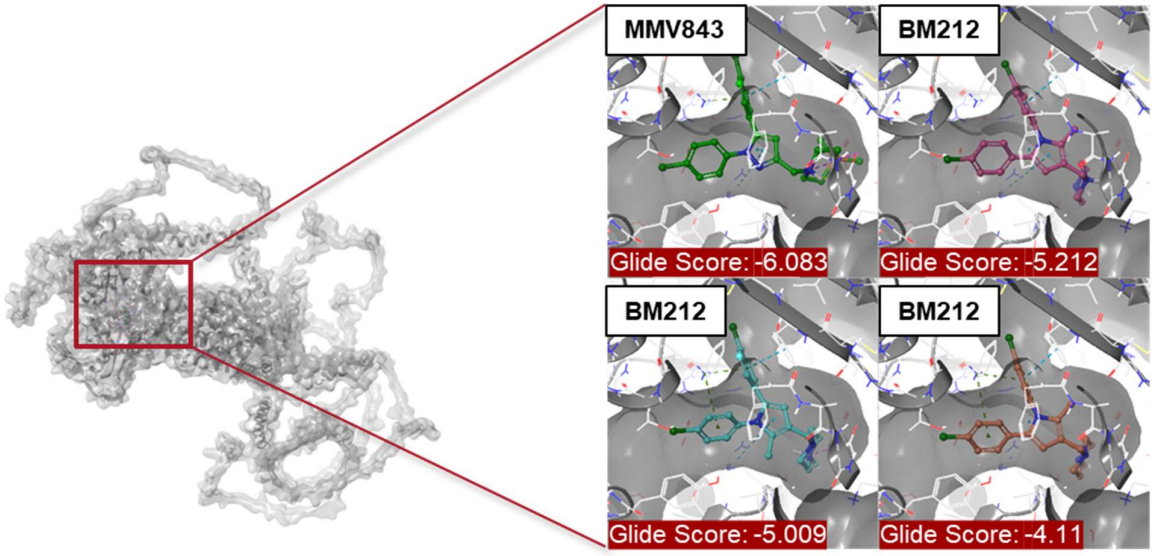

Figure 4.1: Docking poses of MMV843 and its parent compound into Niemann-Pick type C-related protein 1. Docking poses include different tautomeric forms simulated at physiological pH. Most favourable docking poses are presented in inset images. GlideScores are highlighted in maroon blocks. Hydrogen bonds (yellow), halogen bonds (purple), salt bridges (pink), pi-pi stacking (blue) and pi-cation (green) interactions are indicated.

An empirical scoring function, called a GlideScore, approximates the binding free energy of a specified ligand. Good binding is typically represented by GlideScores of -10 or lower; however, scores of -8 or -9 may be acceptable for certain targets (such as those with shallow active sites) [116]. Different systems will have different thresholds for what constitutes a "good" score, and adjusting the van der Waals radii scalings will substantially impact scores [116]. Similar GlideScores were seen for MMV843 and BM212 docked into the *P. falciparum* Niemann-Pick type C-related protein 1, with scores ranging from -4.11 to -6.08, below acceptable cutoffs. Since investigations into the *P. falciparum* Niemann-Pick type C-related protein 1 did not indicate optimal docking/association/interaction with MMV843, the possibility for non-MmpL3 mediated effects of MMV843 on *P. falciparum* was explored.

A novel target search with SEA was used to investigate alternative potential targets for MMV843 in any organism. A list of possible targets was obtained with associated P-values (Table 4.1), indicating the likelihood of target specificity. The top two possible targets, namely replication protein A 70 kDa DNA-binding subunit (P-value = 3.571×10^{-68}) and pre-mRNA-processing factor 19 (P-value = 7.064×10^{-43}), were selected for further investigations.

Table 4.1: Possible targets of MMV843 and associated P-values from SEA investigations.

Target identified	Target name	Description	P-value
RFA1_HUMAN	RPA1	Replication protein A 70 kDa DNA-binding subunit	3.571×10^{-68}
PRP19_YEAST	PRP19	Pre-mRNA-processing factor 19	7.064×10^{-43}
DRD1_BOVIN	DRD1	D(1A) dopamine receptor	1.249×10^{-32}
A0A060INS8_CAPHI	CTSH	Cathepsin H	2.478×10^{-25}
5HT2A_PIG	HTR2A	5-hydroxytryptamine receptor 2A	5.121×10^{-21}
SYMC_HUMAN	MARS1	Methionine--tRNA ligase, cytoplasmic	5.425×10^{-19}

Therefore, homologues of the human replication protein A 70 kDa DNA-binding subunit (accession code: P27694) and yeast pre-mRNA-processing factor 19 (accession code: P32523) were searched for in the *P. falciparum* genome using the BlastP tool in PlasmoDB. Homologues in *Plasmodium* were found, with significant E-values, for both investigated proteins (Table 4.2). These *Plasmodium* homologues, namely replication protein A1 large subunit (E-value = 2×10^{-49}) and pre-mRNA-processing factor 19 (E-value = 2×10^{-21}), were selected for further *in silico* analysis. Both protein structures were obtained from AlphaFold and Schrödinger Maestro (2022-4) was used to dock MMV843 and BM212 into the protein structures (Figure 4.2).

Table 4.2: PlasmoDB protein BLAST results and associated E-values.

	PlasmoDB accession code	Target name	E-value
Replication protein A 70 kDa DNA-binding subunit	PF3D7_0409600	Replication protein A1, large subunit	2×10^{-49}
	PF3D7_0904800	Replication protein A1, small fragment	2×10^{-26}
	PF3D7_0219100	Saccharopine dehydrogenase, putative	2.5
	PF3D7_0616900	Conserved *Plasmodium* protein, unknown function	7.7
	PF3D7_1477300	*Plasmodium* exported protein (PHIST), unknown function	5.4
Pre-mRNA-processing factor 19	PF3D7_0308600	Pre-mRNA-processing factor 19, putative	2×10^{-21}
	PF3D7_0707700	E3 ubiquitin-protein ligase, putative	0.014
	PF3D7_0826500	Ubiquitin conjugation factor E4 B, putative	0.24
	PF3D7_1426300	Dynein intermediate chain, putative	1.3
	PF3D7_0809600	Peptidase family C50, putative	2.4
	PF3D7_1200200	Rifin	5.7

Similar GlideScores of -1.31 to -4.27 were obtained for MMV843 and BM212 docked into *P. falciparum* pre-mRNA-processing factor 19 (Figure 4.2A). Additionally, GlideScores, within the range of -0.95 to -3.29 were obtained for both compounds after docking into *P. falciparum* replication protein A1, large subunit (Figure 4.2B). These GlideScores were all below the acceptable cutoffs. *P. falciparum* pre-mRNA-processing factor 19 and replication protein A1, large subunit are likely not the targets of MMV843 as optimal docking with MMV843 was not indicated for either protein investigated. Since favourable binding of MMV843 and BM212 to the three proteins explored were not found, further interactions between the ligands and the protein residues were not investigated. Therefore, alternative approaches were used to explore the possible MoA of MMV843.

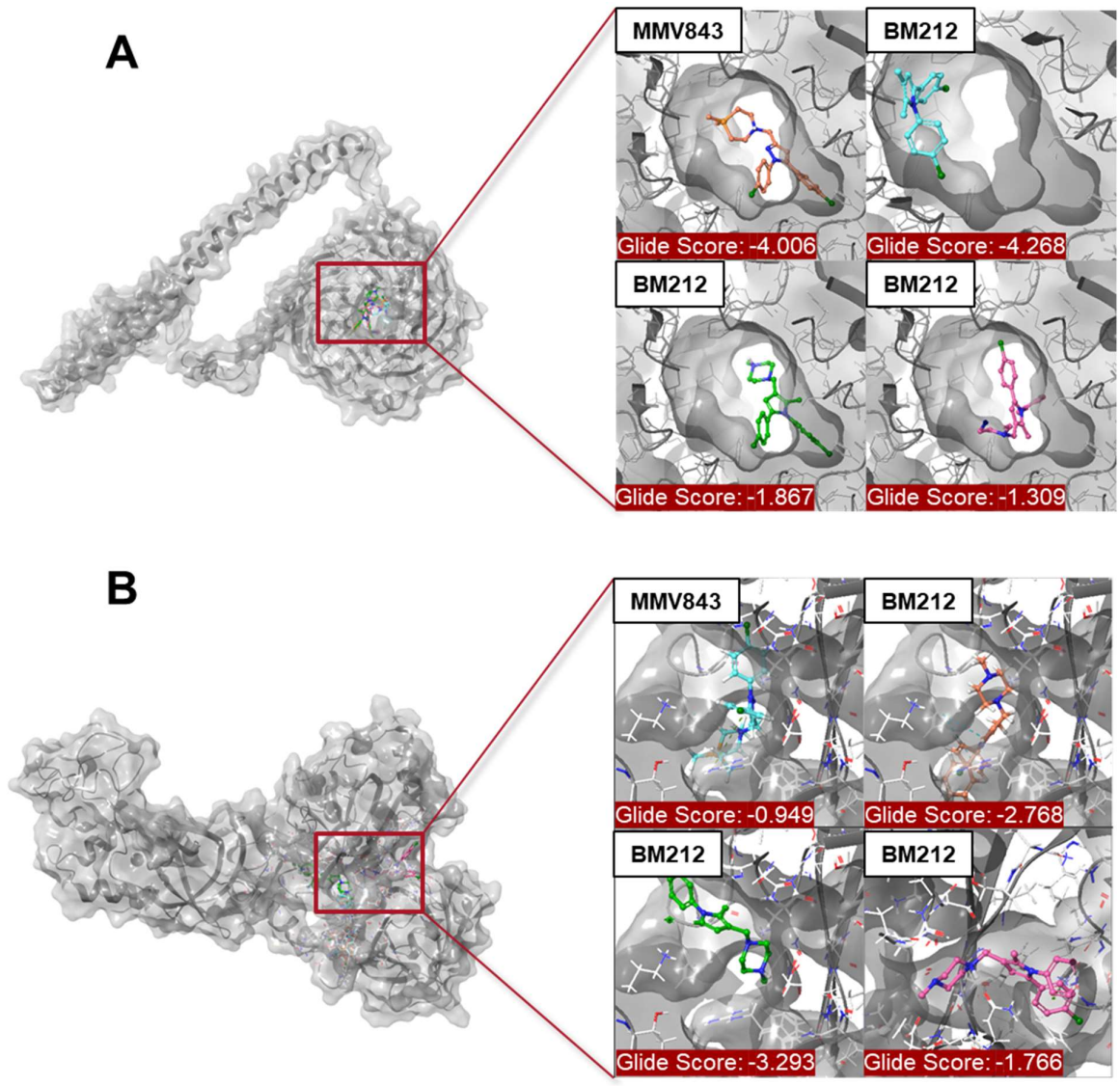

Figure 4.2: Docking poses of MMV843 and its parent compound into selected targets. Docking poses include different tautomeric forms simulated at physiological pH. **(A)** *P. falciparum* pre-mRNA-processing factor 19 **(B)** *P. falciparum* replication protein A1, large subunit. Most favourable docking poses are presented in inset images. GlideScores are highlighted in maroon blocks. Hydrogen bonds (yellow), halogen bonds (purple), salt bridges (pink), pi-pi stacking (blue) and pi-cation (green) interactions are indicated.

4.2. Kinetic/rate of action study

Establishing whether a compound is fast- or slow-acting is an important early step in the drug discovery process to profile a compound's MoA [141]. To evaluate the rate of gametocytocidal action of MMV843, *P. falciparum* late-stage gametocytes were treated at 1x and 5x IC_{50} for four different time points (6, 12, 24 and 48 h), and both gametocytaemia and gametocyte viability were investigated (Figure 4.3). A significant decrease (unpaired, parametric Student's t-test with Welch's correction, $P<0.0001$, n = 3) in gametocytaemia was observed after 6 h of treatment onwards, indicating that the effect was present already within the first 6 h of exposure of gametocytes to MMV843 (Figure 4.3A). This significance was retained for both concentrations and at each time

point. Additionally, gametocyte viability was significantly decreased (unpaired, parametric Student's t-test with Welch's correction, *P*<0.001, n = 3) after only 6 h of treatment (Figure 4.3B), and this significance was again retained throughout, for both concentrations and at each time point. Therefore, MMV843 has rapid parasite-killing kinetics, acting within 6 h of drug exposure.

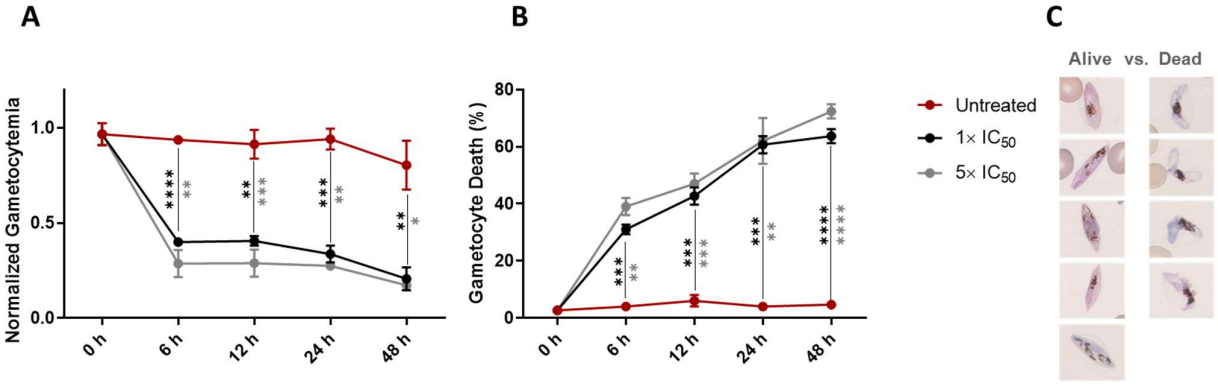

Figure 4.3: Rate of gametocytocidal action of MMV843 against *P. falciparum* late-stage gametocytes. Gametocytes were treated at 117 nM (1x IC_{50}) or 585 nM (5x IC_{50}) and both gametocytaemia **(A)** and gametocyte death **(B)** were determined at 6, 12, 24 and 48 h post-treatment. **(C)** Representative gametocyte images illustrating the distinction between dead and living parasites. Data are from three independent biological repeats (n = 3). An unpaired, parametric Student's t-test with Welch's correction was performed between treated, 1x IC_{50} (indicated in black) and 5x IC_{50} (indicated in grey), and untreated gametocytes at each time point. * = *P*<0.05, ** = *P*<0.01, *** = *P*<0.001 and **** = *P*<0.0001.

4.3. Confocal microscopy of drug-treated late-stage gametocytes

Confocal microscopy of unfixed *P. falciparum* late-stage gametocytes was performed using organelle-specific fluorescent dyes to evaluate the involvement of various biochemical processes in the MoA of MMV843. These fluorophores were used as a tool, allowing the investigation post-treatment on a whole-cell level, both morphologically and biochemically.

4.3.1. JC-1 to investigate drug effects on gametocyte mitochondrial membrane potential

The significance of mitochondria in cellular energy production and metabolic processes underscores their pivotal role in the intricate life cycle of *Plasmodium* and thus presents an attractive target in drug discovery. Therefore, a mitochondrial-specific dye, JC-1, was used to explore the mitochondria as a possible target of MMV843.

The ratio metric dye, JC-1, was used to probe mitochondrial membrane potential with red fluorescence associated with intact mitochondria and aggregated JC-1, or green fluorescence associated with monomeric JC-1 in the cytosol. Gametocytes were treated with MMV843 for 6 h and 24 h at 1x IC_{90} and 2x IC_{50}, respectively, then treated and untreated parasites were stained with JC-1. Additionally, gametocytes were treated with MMV048 (a positive control for cell death with a different MoA) for 24 h at 2x IC_{50} and stained with JC-1. A 6 h treatment with MMV048 was not

included for this compound, having PfPI4K as a validated drug target, was previously shown to only act after 24 h of exposure [125]. Figure 4.4 shows a distinct, punctate red structure and a separate, linearly dispersed red structure in all images of untreated parasites stained with JC-1.

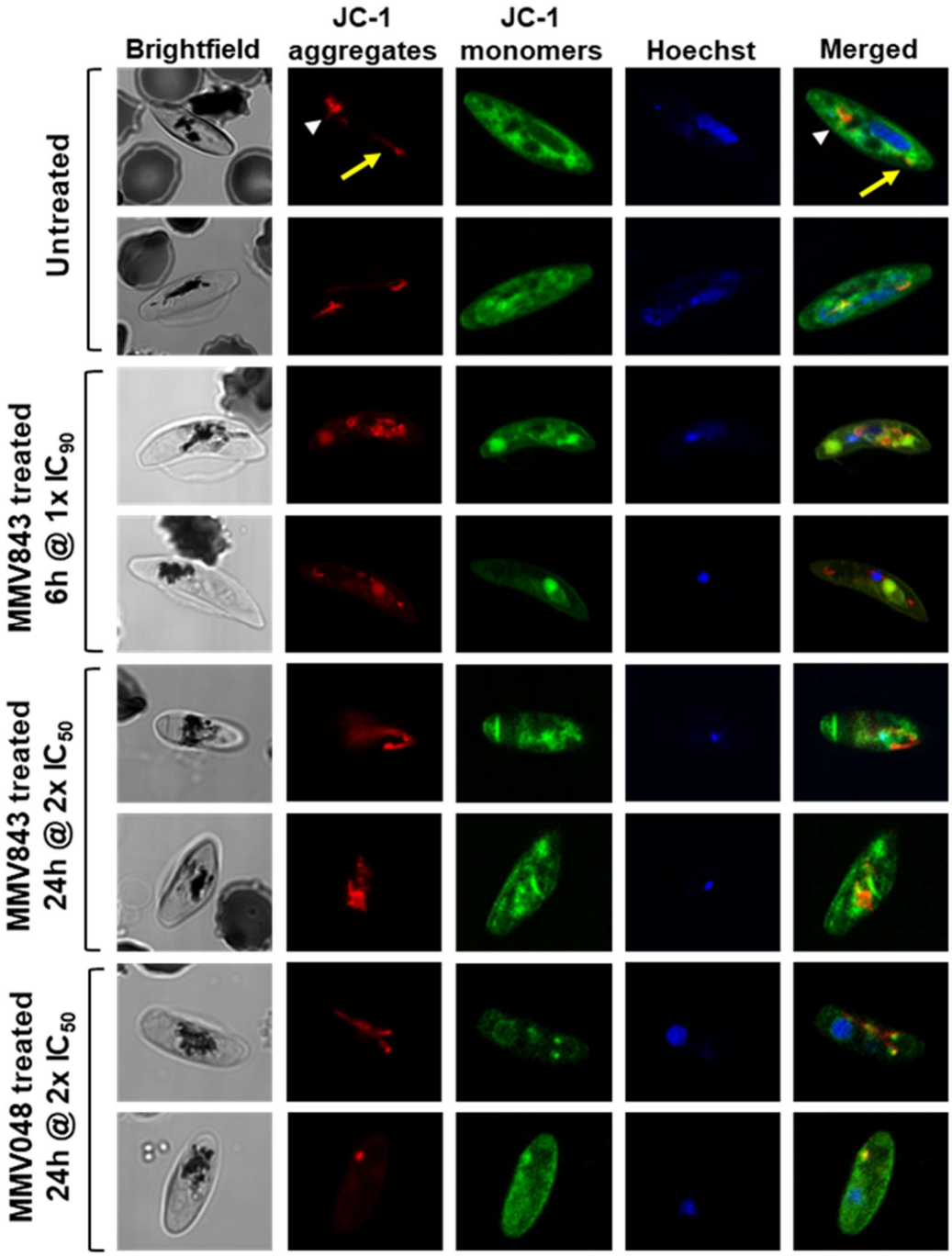

Figure 4.4: Live confocal microscopy visualisation of untreated, MMV843- and MMV048-treated late-stage gametocytes stained with JC-1. Parasites are stained with JC-1, indicating aggregates (red) and monomers (green), and the DNA-specific dye Hoechst (blue). Merged and brightfield images are included. Two representative images are shown for the untreated gametocytes and each drug treatment and time period, namely 6 h treatment with MMV843 (1x IC_{90}), 24 h treatment with MMV843 (2x IC_{50}) and 24 h treatment with MMV048 (2x IC_{50}). Distinct, punctate red structure is indicated by a white arrowhead and the separate linearly dispersed red structure is indicated by a yellow arrow.

Overlaying the red and green signals of the untreated parasites indicated the presence of a punctate red structure and a red-green overlay area – seen as yellow.

Comparing the untreated to the MMV843 parasites treated for 6 h at 1x IC_{90}, numerous strong punctate red structures are seen, in contrast to the untreated population, less distinct red staining is dispersed throughout the gametocytes (Figure 4.4). Overlayed red and green signals show strong punctate red structures and red-green overlay areas are seen as yellow, these are more pronounced in comparison to the untreated overlayed images. For MMV843 parasites treated for 24 h at 2x IC_{50}, strong localized staining is again seen; however, the amount of structures present is less than that seen after the 6 h MMV843 treatment. Additionally, these punctate red structures are larger than those seen in the untreated images. Dispersion of red signal is also observed, and the red-green overlay area is visible, but not as much as is seen for the 6 h MMV843-treated parasites. The gametocytes treated with MMV048 for 24 h at 2x IC_{50} show the same smaller distinct red structures, as seen in the untreated population, and dispersion of red staining is seen. The red-green overlay is visible; however, it is not as pronounced as seen after MMV843 treatment.

The Fiji distribution of ImageJ was used to quantitatively measure mean fluorescent intensity with the region of interest defined as the whole gametocyte cell (Figure 4.5).

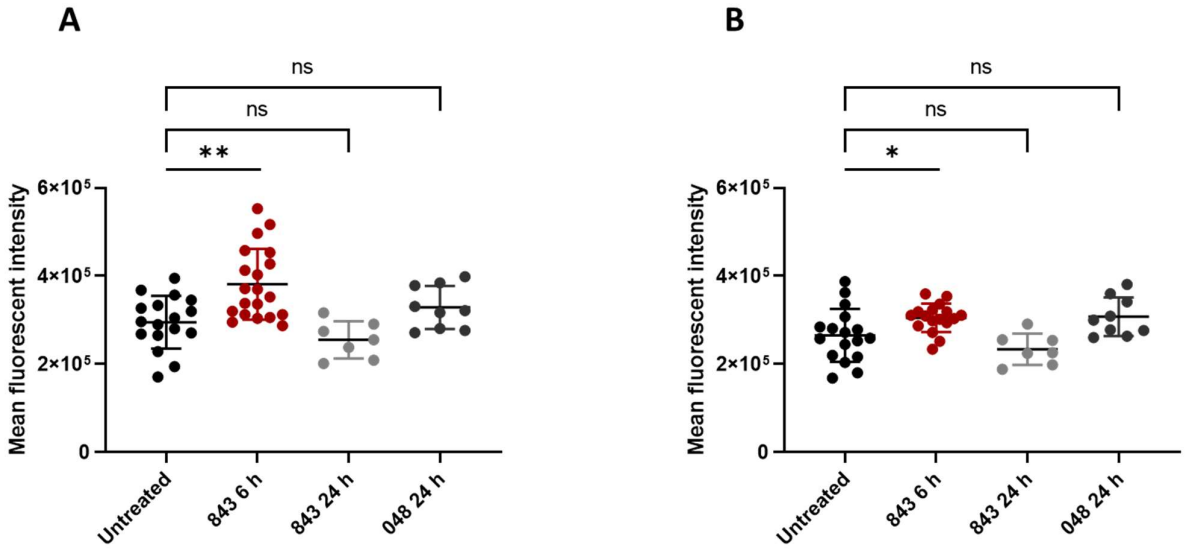

Figure 4.5: Mean fluorescent intensity of JC-1 (A) aggregates and (B) monomers for treated and untreated late-stage gametocytes. The 6 h treatment with MMV843 (1x IC_{90}), 24 h treatment with MMV843 (2x IC_{50}), 24 h treatment with MMV048 (2x IC_{50}) and untreated data are represented. The region of interest was defined as the whole gametocyte cell and the fluorescent intensity of both JC-1 aggregates and monomers was quantified with the Fiji distribution of ImageJ. A non-parametric Mann-Whitney *U* test was performed for all drug treatments and time points compared to the untreated condition. * = $P<0.05$, ** = $P<0.01$ and ns = $P\geq0.05$.

A significant increase (non-parametric Mann-Whitney *U* test, $P<0.01$ and $P<0.05$, n = ≥7) is seen for both the red (Figure 4.5A) and green (Figure 4.5B) fluorescence signals after 6 h of treatment with MMV843 (1x IC_{90}) compared to the untreated. However, there is no dramatic change in red and green signals after a 24 h treatment (2x IC_{50}) with both MMV843 and MMV048 indicative of a dead/dying phenotype after this prolonged drug exposure. Therefore, this data may indicate that MMV843 targets the mitochondria of late-stage gametocytes and affects mitochondrial membrane potential within the first 6 h of exposure.

4.3.2. ER-Tracker to investigate drug effects on the endoplasmic reticulum in gametocytes

The ER is crucial for various cellular processes and applying ER stress can be used to disrupt parasite development [71]. With this in mind, the ER was explored as a possible target of MMV843 using an ER-specific dye, ER-Tracker™ Red.

Gametocytes were treated with MMV843 (6 h and 24 h at 1x IC_{90} and 2x IC_{50}, respectively) and MMV048 (24 h at 2x IC_{50}). Following this, treated and untreated parasites were stained with ER-Tracker Red. Figure 4.6 shows areas of pronounced ER red staining and faintly diffused red signal observed throughout the untreated gametocyte. The 6 h MMV843-treated (1x IC_{90}) parasites present a similar staining pattern to the untreated population, with pronounced structured ER red staining and faint cell-wide dispersion of the red signal. In contrast to both the untreated and 6 h MMV843-treated populations, prominent red staining can be seen throughout the 24 h MMV843-treated (2x IC_{50}) parasites. Similarly, to the 24 h MMV843-treated populations, pronounced cell-wide spreading of the red stain throughout the gametocytes is also observed for MMV048-treated (2x IC_{50}) parasites. This staining pattern seen for 24 h MMV843- and MMV048-treated parasites is indicative of a dead/dying phenotype, potentially due to ER accumulations which may be associated with ER stress, after this prolonged drug exposure.

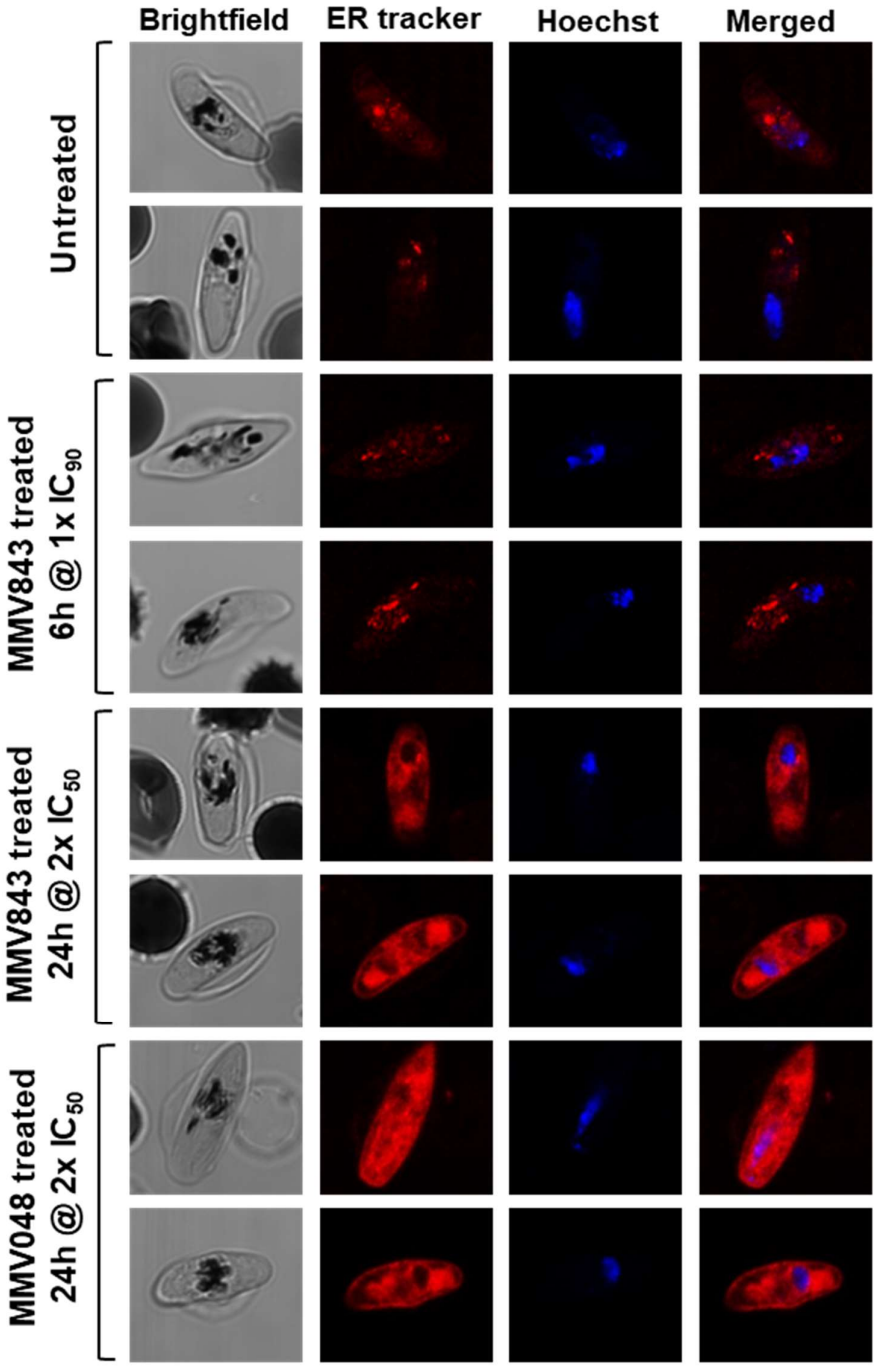

Figure 4.6: Live confocal microscopy visualisation of untreated, MMV843- and MMV048-treated late-stage gametocytes stained with ER-Tracker Red. Parasites are co-stained with ER-Tracker (Red) and the DNA-specific dye Hoechst (blue). Merged and brightfield images are included. Two representative images are shown for the untreated gametocytes and each drug treatment and time period, namely 6 h treatment with MMV843 (1x IC_{90}), 24 h treatment with MMV843 (2x IC_{50}) and 24 h treatment with MMV048 (2x IC_{50}).

As in section 4.3.1., mean fluorescent intensity was quantified for the untreated parasites and specified drug treatments with respective time points (Figure 4.7). There was no significant difference between the fluorescent intensity of the untreated and 6 h MMV843-treated parasites, suggesting that the compound has not affected the ER within the stipulated time. Since MMV843 has been

shown to work within the first 6 h of exposure to the parasites, this points towards the fact that the ER is most likely not involved in the compounds MoA. By contrast, a significant increase (non-parametric Mann-Whitney *U* test, $P<0.01$ and $P<0.001$, n = ≥8) in fluorescent intensity is seen after 24 h treatment with both MMV843 and MMV048 compared to the untreated parasites. Again, this may point to non-specific death/dying phenotypes associated with ER stress resulting in ER accumulations.

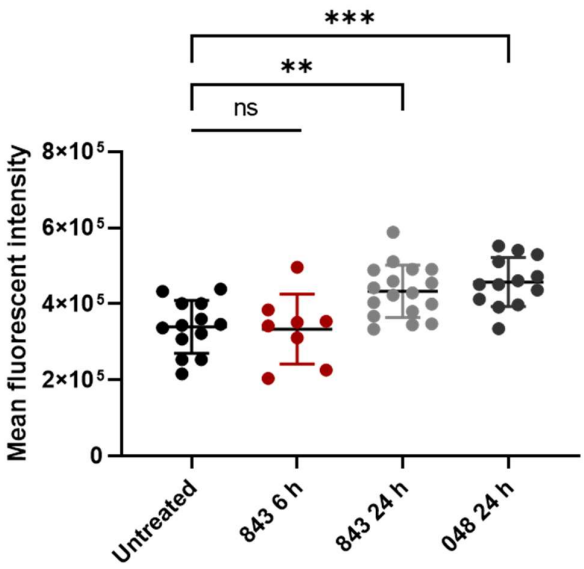

Figure 4.7: Mean fluorescent intensity of ER-Tracker Red for treated and untreated late-stage gametocytes. The 6 h treatment with MMV843 (1x IC_{90}), 24 h treatment with MMV843 (2x IC_{50}), 24 h treatment with MMV048 (2x IC_{50}) and untreated data are represented. Fluorescent intensity of the ER staining was quantified with the Fiji distribution of ImageJ. A non-parametric Mann-Whitney *U* test was performed for all drug treatments and time points compared to the untreated condition. ** = $P<0.01$, *** = $P<0.001$ and ns = $P\geq0.05$.

4.3.3. BODIPY-TR-ceramide to investigate drug effects on gametocyte membranes

As discussed, the parent compounds (rimonabant and BM212) of MMV843 have been shown to directly target MmpL3 in *Mycobacterium tuberculosis* [56, 59]. Investigation into the *P. falciparum* genome for MmpL3-like targets showed no direct homologues to MmpL3 [54]. However, the *P. falciparum* Niemann-Pick type C-related protein 1 (a parasite plasma membrane lipid transporter) is part of the same superfamily as MmpL3, namely the RND-superfamily. The Niemann-Pick type C-related protein 1 is a druggable target required for the maintenance of the appropriate parasite membrane lipid composition and thus homeostasis [140]. Although *in silico* investigations did not indicate optimal docking of MMV843 into the Niemann-Pick type C-related protein 1, parasite membrane domains were further explored as a possible target of MMV843 using the ceramide analogue, BODIPY-TR-ceramide.

Gametocytes were treated with MMV843 (6 h and 24 h at 1x IC_{90} and 2x IC_{50}, respectively) and MMV048 (24 h at 2x IC_{50}), followed by BODIPY-TR-ceramide staining. In untreated parasites,

dispersed red fluorescent staining is observed, with increased staining at the gametocyte membrane as expected (Figure 4.8). Treatment with MMV843 (1x IC_{90}) for 6 h appears to result in a similar staining profile as the untreated parasites although other/increased vesicular staining is present that could indicate redistribution of lipid content in these parasites. Increased red staining of the membrane and diffusion of red fluorescence throughout the cell is seen after 24 h treatment with MMV843 (2x IC_{50}). In contrast to the staining pattern seen for untreated and 6 h MMV843-treated parasites, treatment with MMV843 for 24 h shows a more pronounced diffusion of red fluorescence cell-wide. Images taken after 24 h MMV048 treatment indicate a much clearer membrane staining profile and reduced cytosolic red fluorescence compared to the untreated and MMV843-treated parasites.

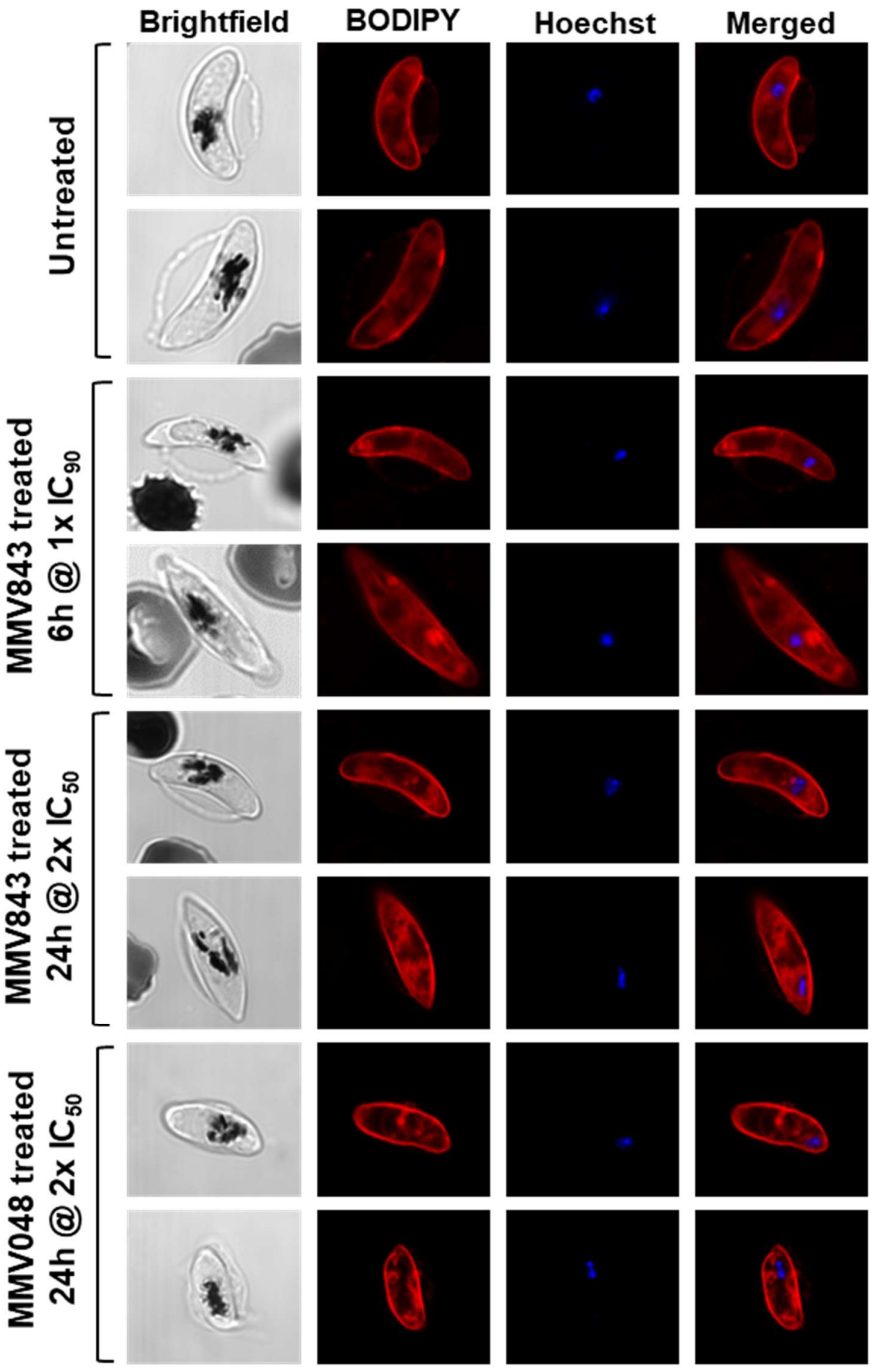

Figure 4.8: Live confocal microscopy visualisation of untreated, MMV843- and MMV048-treated late-stage gametocytes stained with BODIPY-TR-ceramide. Parasites are co-stained with BODIPY-TR-ceramide (Red) and the DNA-specific dye Hoechst (blue). Merged and brightfield images are included. Two representative images are shown for the untreated gametocytes and each drug treatment and time period, namely 6 h treatment with MMV843 (1x IC_{90}), 24 h treatment with MMV843 (2x IC_{50}) and 24 h treatment with MMV048 (2x IC_{50}).

After quantitative investigations of the mean fluorescent intensity, 24 h MMV843-treated parasites were shown to have a significant increase (non-parametric Mann-Whitney *U* test, $P<0.0001$, n = ≥7) in red fluorescence when compared to the untreated population (Figure 4.9). In contrast, the 6 h

MMV843-treated and 24 h MMV048-treated parasites have no significant increase in fluorescence when compared to the untreated parasites. This increase in fluorescence intensity for the 24 h MMV843-treated parasites may be due to downstream effects after drug treatment.

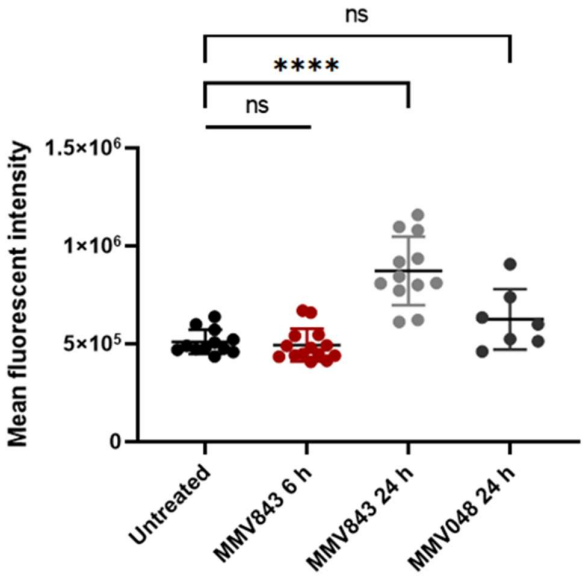

Figure 4.9: Mean fluorescent intensity of BODIPY-TR-ceramide for treated and untreated late-stage gametocytes. The 6 h treatment with MMV843 (1x IC_{90}), 24 h treatment with MMV843 (2x IC_{50}), 24 h treatment with MMV048 (2x IC_{50}) and untreated data are represented. Fluorescent intensity of the BODIPY-TR-ceramide staining was quantified with the Fiji distribution of ImageJ. A non-parametric Mann-Whitney *U* test was performed for all drug treatments and time points compared to the untreated condition. **** = $P<0.0001$ and ns = $P\geq0.05$.

4.3.4. LysoTracker to investigate drug effects on acidic organelles in gametocytes

Given the unique and vital processes that take place in this organelle, the FV of the malaria parasite is an established target for several antimalarials, and thus houses transporters associated with drug resistance [94]. Considering the aforementioned, acidic organelles (i.e. the FV) were investigated as a possible target of MMV843 using LysoTracker™ Red.

Late-stage gametocytes, including untreated parasites, 6 h and 24 h MMV843-treated and 24 h MMV048-treated parasites, were stained with LysoTracker (Figure 4.10). Untreated parasites stained with LysoTracker show a localization of distinct, punctate red staining with a faint red signal seen throughout the rest of the parasite. In comparison, after 6 h treatment with MMV843 (1x IC_{90}) areas of distinct red staining are seen, yet this area of increased signal is more dispersed compared to the untreated population. Additionally, the cell-wide faint red signal seen for the untreated parasites is more granulated after the 6 h MMV843 treatment.

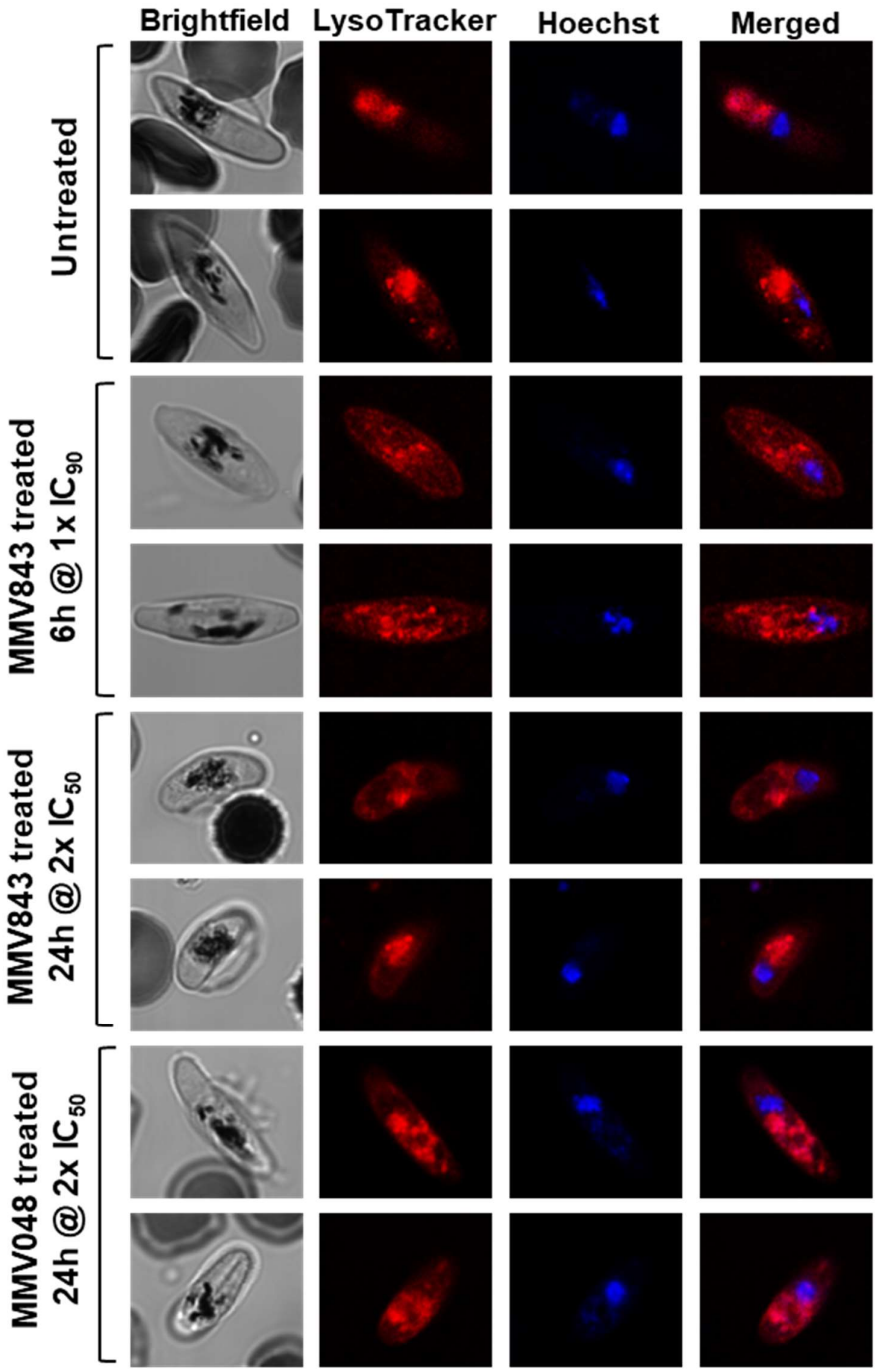

Figure 4.10: Live confocal microscopy visualisation of untreated, MMV843- and MMV048-treated late-stage gametocytes stained with LysoTracker. Parasites are co-stained with LysoTracker (Red) and the DNA-specific dye Hoechst (blue). Merged and brightfield images are included. Two representative images are shown for the untreated gametocytes and each drug treatment and time period, namely 6 h treatment with MMV843 (1x IC_{90}), 24 h treatment with MMV843 (2x IC_{50}) and 24 h treatment with MMV048 (2x IC_{50}).

Following 24 h treatment with MMV843 (2x IC_{50}), again the distinct punctate staining is seen, being more localized (as observed in untreated parasites) compared to the 6 h MMV843 treatment. However, this area of increased staining is smaller than that seen in the untreated parasites. A fainter

staining pattern is observed throughout the rest of the cell. The staining pattern of the 6 h MMV843-treated and 24 h MMV048-treated (2x IC_{50}) parasites is similar, with the area of increased signal being more dispersed compared to the untreated population. In contrast to the 6 h MMV843 treatment, the gametocyte-wide faint red signal seen is not as granulated after 24 h treatment with MMV048.

No dramatic difference (non-parametric Mann-Whitney *U* test, $P<0.05$ and $P<0.01$, n = ≥10) in mean fluorescent intensity was observed between the untreated and treated gametocytes after quantitative analysis (Figure 4.11). However, it should be noted that although the change in mean fluorescent intensity might be non-significant, differing staining patterns are seen between the untreated and treated parasites. The distinct, punctate red staining is more localised in the untreated parasites compared to the 6 h MMV843-treated, which is more dispersed.

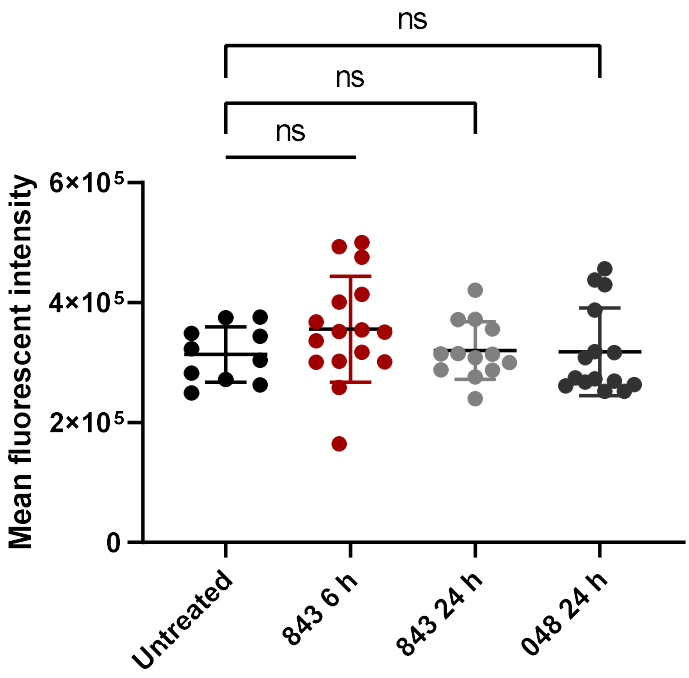

Figure 4.11: Mean fluorescent intensity of LysoTracker for treated and untreated late-stage gametocytes. The 6 h treatment with MMV843 (1x IC_{90}), 24 h treatment with MMV843 (2x IC_{50}), 24 h treatment with MMV048 (2x IC_{50}) and untreated data are represented. Fluorescent intensity of the LysoTracker staining was quantified with the Fiji distribution of ImageJ. A non-parametric Mann-Whitney *U* test was performed for all drug treatments and time points compared to the untreated condition. ns = $P\geq0.05$.

4.4. Determining the IC_{50} of known antimalarials for downstream investigations

To further explore the MoA of MMV843 in downstream experiments, the IC_{50} of known antimalarials, with validated drug targets, needed to be established. Although MMV843 has potent activity against

late-stage *P. falciparum* gametocytes, the compound's activity against the ABS parasites is extremely low. Therefore, the ABS active derivative of MMV843, CL268, was used as a proxy. The activity of CL268, as well as four known antimalarials, with validated drug targets (atovaquone (cytochrome bc1 (Q_0)), KAF156 (protein secretory pathway), P218 (DNA replication/transcription) and MMV048 (PfPI4K)), was determined against ring-stage ABS parasites (Table 4.3). CL268 exhibited an IC_{50} of ~400 nM (Figure 4.12), similar to that obtained by researchers in the M^2PL lab (487 ± 73.8 nM, Dr M van der Watt, personal communication). The determined IC_{50} of the four known antimalarials is comparative to that found in literature [125, 138, 142, 143].

Table 4.3: IC_{50}'s obtained for CL268 and four known antimalarials against ring-stage asexual *P. falciparum* parasites

Compounds investigated	Mean IC_{50} ± S.E.
CL268	409.9 ± 7.2 nM
Atovaquone	0.077 ± 0.006 nM
MMV390048	31.1 ± 3.4 nM
KAF156 (Ganaplacide)	5.06 ± 0.13 nM
P218	0.6457 ± 0.0005 nM

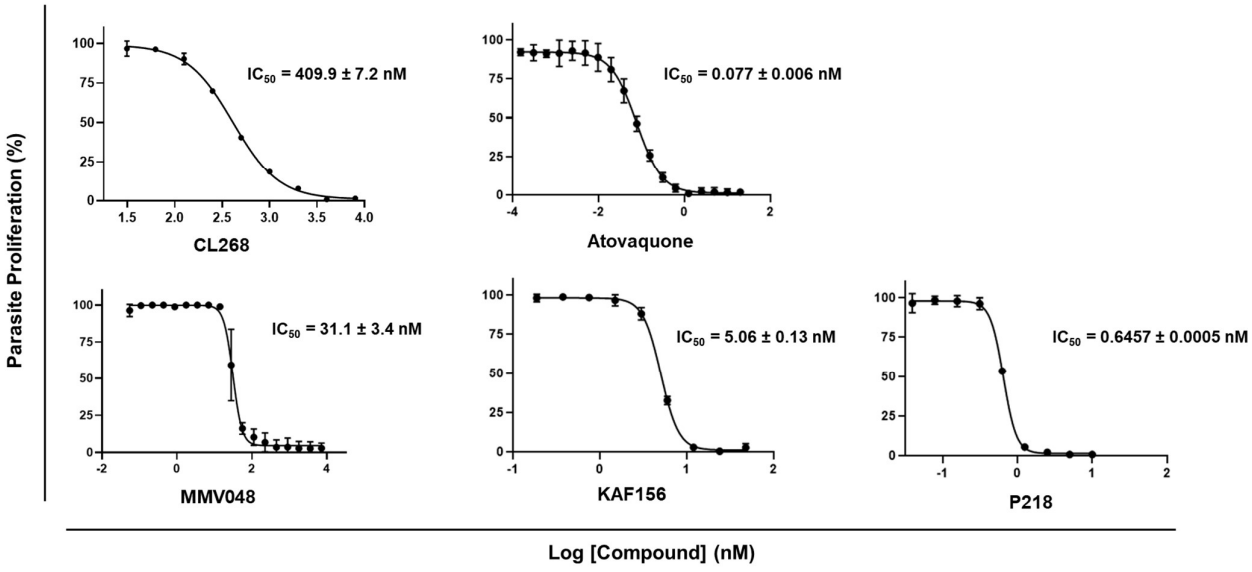

Figure 4.12: Dose-response curves of CL268 and four known antimalarials against ring-stage asexual *P. falciparum* parasites. Non-linear regression curves were generated using GraphPad Prism 8.0 software. IC_{50} values for each compound are indicated. Data are from three independent biological repeats (n = 3), performed in technical triplicate, mean ± SE indicated as error bars for each individual datapoint.

4.5. IC_{50} shift assays as tools to further investigate MoA

Further investigations into the possible targets of MMV843 was performed by determining cross reactivity of CL268 (the proxy for MMV843) to known antimalarials with validated drug targets to test for the possible potentiation of drug effect. The IC_{50} values obtained in section 4.4 (Figure 4.13) were used to perform IC_{50} shifts, involving the treatment of CL268 in combination with each known antimalarial against ring-stage ABS parasites.

Figure 4.13A displays a significant 4-fold shift (unpaired, parametric Student's t-test, $P<0.001$, n = 3) in IC_{50} seen between parasites treated with CL268 alone (~460 nM) and those treated with CL268 in combination with atovaquone (~100 nM). This substantial shift indicates that atovaquone potentiates CL268's effect; however, whether this is due to additive or synergistic effects cannot be confirmed without further isobole analysis. No shifts were observed with the remaining three antimalarials (MMV048, KAF156 and P218) in combination with CL268 (Figure 4.13B-D).

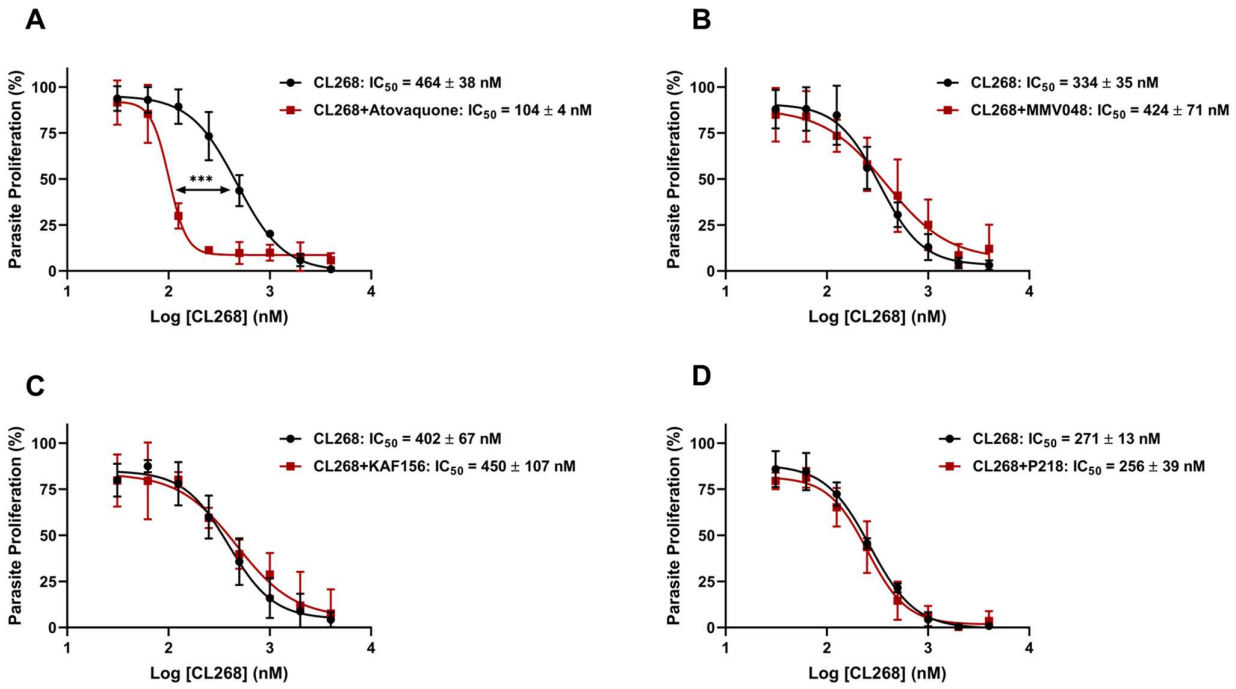

Figure 4.13: Dose-response curves of CL268 in combination with known antimalarials against ring-stage asexual *P. falciparum* parasites. Non-linear regression curves were generated using GraphPad Prism 8.0 software. IC_{50} values for each compound are indicated. Data are from three independent biological repeats (n = 3), performed in technical triplicate, mean ± SE indicated as error bars for each individual datapoint. An unpaired, parametric Student's t-test was performed between parasites treated with CL268 alone and parasites treated with CL268 in combination with atovaquone. *** = $P<0.001$.

5. Discussion

Malaria remains a significant global health concern, and the emergence of antimalarial resistance poses a substantial threat to existing therapeutic interventions. Blocking transmission is essential for malaria elimination, given that current drugs primarily target ABS parasites and liver stages. These drugs either reduce the severity of clinical infection or protect individuals from infection, respectively [30]. The lower number and non-replicating characteristics of gametocytes render the development of resistance to transmission-blocking, gametocyte-specific antimalarials highly improbable. Consequently, there has been a shift in focus towards transmission-blocking drugs, aiming to prevent the spread of the parasite and eliminate the risk of infection [31]. Gametocyte-specific antimalarials are presumed to target unique biological processes compared to compounds targeting ABS parasites, reflecting the fundamental difference in the biology associated with ABS proliferation and gametocyte differentiation. ABS parasites exhibit fermentative metabolism, characterized by increased metabolic flux through glycolysis and the induction of the Warburg effect [45, 144]. In contrast, gametocytes do not undergo DNA replication or nuclear division [46], and a shift to oxidative metabolism is observed [47, 145].

This study aimed to determine the organelles implicated in the MoA of MMV843 against late-stage gametocytes through biochemical approaches. MMV843, the derivative of rimonabant and BM212, is a unique chemotype that is structurally distinct from any current antimalarial and has potent transmission-blocking activity [54]. Understanding the MoA of antimalarial drugs is paramount in the drug discovery process and acceleration thereof since novel antimalarials with unique MoA that may exhibit high barriers to resistance development are crucially needed [53]. While current target identification strategies predominantly focus on the ABS of the parasite life cycle, there is a noticeable gap in knowledge regarding the MoA of gametocyte-specific antimalarials. Additionally, this study proposes that exploiting the unique biology of gametocytes could offer valuable insights into the MoA of antimalarials specifically targeting this stage. Recognizing the marked differences between the biology of ABS parasites and gametocytes, this study has introduced a novel approach focused on using organelle-specific dyes to evaluate the involvement of various biochemical processes in the MoA of MMV843. This method was based on the Cell Painting technique and thus used fluorescent indicators to elucidate comprehensive morphological and biochemical alterations occurring on a whole-cell level.

This study represents one of the first pieces of evidence supporting the use of morphological profiling to elucidate the MoA of gametocyte-specific compounds. These findings provide convincing data, comparable to or potentially indicative of Cell Painting as a feasible methodology for future application in *Plasmodium*. The successful use of individual stains presented here makes attempting multiplexing of several fluorescent dyes, to simultaneously study relevant cellular components and organelles, a plausible strategy in the future. Additionally, high-resolution techniques, such as expansion microscopy or super-resolution fluorescence microscopy, could offer valuable insights

into parasite organization in three dimensions. Future studies should incorporate z-stacking into confocal microscopy investigations. Z-stacking yields a composite image with a more profound depth of field, compared to individual source images, achieved by combining numerous images captured at different focal distances. The quantitative data obtained will allow different parameters to be investigated and not just look at overall fluorescent intensity.

The data presented in this study points towards the mitochondria of late-stage gametocytes being a target of MMV843. Here, the mitochondrial-specific dye, JC-1, was used to explore the mitochondria as a possible target of MMV843. A significant increase in both red (JC-1 aggregates) and green (JC-1 monomers) fluorescence signal was observed after a 6 h treatment with MMV843 (1x IC_{90}), compared to the untreated parasites. This correlates with the rate of action study findings, which demonstrated the rapid parasite-killing kinetics of MMV843. The significant reduction in both gametocytaemia and gametocyte viability within 6 h of drug exposure to the gametocytes supports the rapid efficacy of this compound. This fast action may be because either the target is readily available, or the target is essential in gametocytes. In contrast to ABS parasites, gametocyte mitochondria exhibit an expanded and elongated morphology, featuring the development of multiple tubular cristate structures [146, 147], reflecting the activation of mitochondrial metabolism in these stages [148]. Furthermore, a drastic decrease in glycolysis is observed, with energy production reliant on oxidative metabolism via the tricarboxylic acid (TCA) cycle [145, 149]. The effect of a drug combination with atovaquone was explored to further investigate the mitochondria as the potential target of MMV843. Atovaquone is a competitive inhibitor of the mitochondrial cytochrome bc1 complex's quinol oxidation (Q_o) site. When this enzyme is inhibited after atovaquone treatment, pyrimidine production is disrupted, the mitochondrial membrane potential collapses, and the parasite dies as a result [150]. Although MMV843 has potent activity against late-stage *P. falciparum* gametocytes, the compound's activity against the ABS parasites is extremely low. Therefore, a derivative of MMV843, namely CL268, was used as a proxy since its activity against ABS parasites is good. The target of CL268 is also unknown but assumed to have a similar target to MMV843. In addition to the expanded mitochondria seen in gametocytes, the activity of mitochondrial cytochrome b is increased by 7-fold in these stages [151]. This is interesting since we have shown that the addition of atovaquone potentiated the effect of CL268 (the proxy for MMV843), displaying a significant 4-fold decrease in IC_{50}. However, whether this is due to additive or synergistic effects cannot be confirmed without further isobole analysis. The lack of IC_{50} shifts observed with KAF156, P218 and MMV048 further supports the potentiating effects exhibited with atovaquone. Therefore, this data may indicate that MMV843 targets the mitochondria of late-stage gametocytes and affects mitochondrial membrane potential within the first 6 h of exposure.

In this study, we additionally investigated alternative vital components in gametocytes, including the ER, membrane structures and the FV, using organelles-specific dyes to visualize these structures following drug treatment. No significant difference between the fluorescent intensity of the untreated

and 6 h MMV843-treated parasites was observed, suggesting that the compound did not affect the ER within the stipulated time. Since MMV843 has been shown to act within the first 6 h of exposure to the parasites, this points towards the fact that the ER is most likely not the compound's target. By contrast, a significant increase in fluorescent intensity is seen after 24 h treatment with both MMV843 and MMV048 compared to the untreated parasites. Again, this may point to non-specific death/dying phenotypes associated with ER stress resulting in ER accumulations. These ER accumulations have been described in gametocytes as functional subdivisions of the ER, characterized as large, intricate, and dense ER tubule networks, which may be associated with ER stress [71]. Investigations into gametocyte membrane domains showed increased red staining of the membrane and diffusion of red fluorescence throughout the cell after 24 h treatment with MMV843, significant compared to the untreated and 6 h treated parasites. The data here show that the gametocyte mitochondria are a putative target of MMV843, which can now be further validated as such. Although *in silico* investigations did not indicate optimal docking of MMV843 into the Niemann-Pick type C-related protein 1 (a parasite plasma membrane lipid transporter), docking faces significant limitations. These limitations include inadequate sampling of ligand and receptor conformations in pose prediction and the utilization of estimated scoring functions, often yielding results inconsistent with experimental binding affinities [152, 153]. The poor binding modes for this protein, generated by molecular docking simulations, may also be attributable to the lack of a solved structure such as cryo-EM derived crystal structures. Thus, it is plausible that the membrane is an additional target of the investigated compound. Although no dramatic difference in mean fluorescent intensity was observed between the untreated and treated gametocytes, following staining of the gametocyte FV, differing staining patterns were seen. The distinct, punctate red staining of the FV was more localised in the untreated parasites compared to the 6 h MMV843-treated parasite FVs, which was more dispersed. The FV is an acidic lysosome-like organelle in gametocytes and may function as a sensitive indicator of cellular stress, similar to eukaryote lysosomes [154]. In eukaryotes, lysosomal membrane destabilization leading to cell death has been linked to various stress stimuli, including oxidative stress [155-157]. Following drug exposure, the *Plasmodium* FV may be permeabilized resulting in the contents leaking out and acidifying the cytosol [158]. This could explain the dispersed staining pattern seen with LysoTracker, which stains acidic organelles, after drug exposure and can possibly be attributed to a non-specific stress response.

The results of this research present a promising step forward in elucidating the MoA of gametocyte-specific antimalarials, providing a foundation for the development of targeted interventions to disrupt the transmission of malaria. By bridging the existing gap in knowledge and proposing innovative strategies, this study contributes to the ongoing efforts in the global fight against malaria and reinforces the importance of tailored strategies for diverse stages of the parasite life cycle.

6. Conclusion

The emergence of antimalarial resistance poses a substantial threat to existing therapeutic interventions, emphasizing the crucial need for novel antimalarials, particularly those addressing disease transmission by targeting late-stage gametocytes. An important step in the drug discovery process is understanding a compound's MoA. This study showed that our hypothesis could be accepted and that cell-based fluorescent indicators successfully revealed the target of a transmission-selective compound.

Investigations involving fluorescent organelle markers and cross-reactivity studies with known antimalarials point towards the mitochondria of late-stage gametocytes being the possible target of MMV843. We provide evidence of a visualization tool that can form part of a 'tool kit' to understand the MoA of antimalarials and thereby contribute to much needed advances in antimalarial drug discovery.

7. References

1. Verra, F., et al., *A systematic review of transfusion-transmitted malaria in non-endemic areas.* Malar J, 2018. **17**(1): p. 36.
2. Lee, A.H., L.S. Symington, and D.A. Fidock, *DNA repair mechanisms and their biological roles in the malaria parasite Plasmodium falciparum.* Microbiol Mol Biol Rev, 2014. **78**(3): p. 469-86.
3. Antinori, S., et al., *Biology of human malaria plasmodia including Plasmodium knowlesi.* Mediterr J Hematol Infect Dis, 2012. **4**(1): p. e2012013.
4. Ngotho, P., et al., *Revisiting gametocyte biology in malaria parasites.* FEMS Microbiol Rev, 2019. **43**(4): p. 401-414.
5. Gomes, P.S., et al., *Immune Escape Strategies of Malaria Parasites.* Front Microbiol, 2016. **7**: p. 1617.
6. World Health Organization. *World malaria report 2022. Geneva: World Health Organization; 2022. Licence: CC BY-NC-SA 3.0 IGO.* 2022; Available from: https://www.who.int/teams/global-malaria-programme/reports/world-malaria-report-2022.
7. Garrido-Cardenas, J.A., et al., *Plasmodium genomics: an approach for learning about and ending human malaria.* Parasitol Res, 2019. **118**(1): p. 1-27.
8. Centers for Disease Control and Prevention. *Malaria's Impact Worldwide*. 2021; Available from: https://www.cdc.gov/malaria/malaria_worldwide/impact.html.
9. Wassmer, S.C., et al., *Investigating the Pathogenesis of Severe Malaria: A Multidisciplinary and Cross-Geographical Approach.* Am J Trop Med Hyg, 2015. **93**(3 Suppl): p. 42-56.
10. Wassmer, S.C. and G.E. Grau, *Severe malaria: what's new on the pathogenesis front?* Int J Parasitol, 2017. **47**(2-3): p. 145-152.
11. Phillips, M.A., et al., *Malaria.* Nature Reviews Disease Primers, 2017. **3**(1): p. 17050.
12. Ross, L.S. and D.A. Fidock, *Elucidating Mechanisms of Drug-Resistant Plasmodium falciparum.* Cell Host Microbe, 2019. **26**(1): p. 35-47.
13. Soulard, V., et al., *Plasmodium falciparum full life cycle and Plasmodium ovale liver stages in humanized mice.* Nat Commun, 2015. **6**: p. 7690.
14. Renia, L. and Y.S. Goh, *Malaria Parasites: The Great Escape.* Front Immunol, 2016. **7**: p. 463.
15. Kuehn, A. and G. Pradel, *The coming-out of malaria gametocytes.* J Biomed Biotechnol, 2010. **2010**: p. 976827.
16. Venugopal, K., et al., *Plasmodium asexual growth and sexual development in the haematopoietic niche of the host.* Nat Rev Microbiol, 2020. **18**(3): p. 177-189.
17. Meibalan, E. and M. Marti, *Biology of Malaria Transmission.* Cold Spring Harb Perspect Med, 2017. **7**(3).
18. Rueda-Zubiaurre, A., et al., *Structure-Activity Relationship Studies of a Novel Class of Transmission Blocking Antimalarials Targeting Male Gametes.* J Med Chem, 2020. **63**(5): p. 2240-2262.
19. Alout, H., et al., *Malaria Vector Control Still Matters despite Insecticide Resistance.* Trends Parasitol, 2017. **33**(8): p. 610-618.
20. Lobo, N.F., et al., *Modern Vector Control.* Cold Spring Harb Perspect Med, 2018. **8**(1).
21. Siddiqui, A.J., J. Bhardwaj, and S.K. Puri, *mRNA expression of cytokines and its impact on outcomes after infection with lethal and nonlethal Plasmodium vinckei parasites.* Parasitol Res, 2012. **110**(4): p. 1517-24.
22. Aly, A.S., A.M. Vaughan, and S.H. Kappe, *Malaria parasite development in the mosquito and infection of the mammalian host.* Annu Rev Microbiol, 2009. **63**: p. 195-221.
23. Duffy, P.E., et al., *Pre-erythrocytic malaria vaccines: identifying the targets.* Expert Rev Vaccines, 2012. **11**(10): p. 1261-80.
24. Nadeem, A.Y., et al., *Mosquirix RTS, S/AS01 Vaccine Development, Immunogenicity, and Efficacy.* Vaccines (Basel), 2022. **10**(5).
25. Datoo, M.S., et al., *Efficacy of a low-dose candidate malaria vaccine, R21 in adjuvant Matrix-M, with seasonal administration to children in Burkina Faso: a randomised controlled trial.* Lancet, 2021. **397**(10287): p. 1809-1818.

26. Verlinden, B.K., A. Louw, and L.M. Birkholtz, *Resisting resistance: is there a solution for malaria?* Expert Opin Drug Discov, 2016. **11**(4): p. 395-406.
27. Dondorp, A.M., et al., *Artemisinin resistance in Plasmodium falciparum malaria.* N Engl J Med, 2009. **361**(5): p. 455-67.
28. Phyo, A.P., et al., *Emergence of artemisinin-resistant malaria on the western border of Thailand: a longitudinal study.* Lancet, 2012. **379**(9830): p. 1960-6.
29. Miller, L.H., et al., *Malaria biology and disease pathogenesis: insights for new treatments.* Nat Med, 2013. **19**(2): p. 156-67.
30. Wang, J., et al., *Characterization of Pb51 in Plasmodium berghei as a malaria vaccine candidate targeting both asexual erythrocytic proliferation and transmission.* Malar J, 2017. **16**(1): p. 458.
31. Kaslow, D.C., *Transmission-blocking vaccines.* Chem Immunol, 2002. **80**: p. 287-307.
32. Burrows, J.N., et al., *New developments in anti-malarial target candidate and product profiles.* Malar J, 2017. **16**(1): p. 26.
33. Yahiya, S., et al., *The antimalarial screening landscape-looking beyond the asexual blood stage.* Curr Opin Chem Biol, 2019. **50**: p. 1-9.
34. Burrows, J.N., et al., *Designing the next generation of medicines for malaria control and eradication.* Malar J, 2013. **12**: p. 187.
35. Medicines for Malaria Venture. *Target Product Profiles & Target Candidate Profiles*. 2023; Available from: https://www.mmv.org/research-development/information-scientists/target-product-profiles-target-candidate-profiles.
36. Yang, T., et al., *MalDA, Accelerating Malaria Drug Discovery.* Trends Parasitol, 2021. **37**(6): p. 493-507.
37. Smith, R.C., J. Vega-Rodriguez, and M. Jacobs-Lorena, *The Plasmodium bottleneck: malaria parasite losses in the mosquito vector.* Mem Inst Oswaldo Cruz, 2014. **109**(5): p. 644-61.
38. Wadi, I., et al., *Critical examination of approaches exploited to assess the effectiveness of transmission-blocking drugs for malaria.* Future Med Chem, 2018. **10**(22): p. 2619-2639.
39. Yu, S., et al., *Transmission-Blocking Strategies Against Malaria Parasites During Their Mosquito Stages.* Front Cell Infect Microbiol, 2022. **12**: p. 820650.
40. Delves, M., et al., *The activities of current antimalarial drugs on the life cycle stages of Plasmodium: a comparative study with human and rodent parasites.* PLoS Med, 2012. **9**(2): p. e1001169.
41. Medicines for Malaria Venture. *MMV's pipeline of antimalarial drugs*. 2023; Available from: https://www.mmv.org/mmv-pipeline-antimalarial-drugs.
42. Diagana, T.T., *Supporting malaria elimination with 21st century antimalarial agent drug discovery.* Drug Discov Today, 2015. **20**(10): p. 1265-70.
43. Siqueira-Neto, J.L., et al., *Antimalarial drug discovery: progress and approaches.* Nat Rev Drug Discov, 2023. **22**(10): p. 807-826.
44. Chahine, Z. and K.G. Le Roch, *Decrypting the complexity of the human malaria parasite biology through systems biology approaches.* Frontiers in Systems Biology, 2022. **2**.
45. van der Watt, M.E., J. Reader, and L.M. Birkholtz, *Adapt or Die: Targeting Unique Transmission-Stage Biology for Malaria Elimination.* Front Cell Infect Microbiol, 2022. **12**: p. 901971.
46. Dixon, M.W.A. and L. Tilley, *Plasmodium falciparum goes bananas for sex.* Mol Biochem Parasitol, 2021. **244**: p. 111385.
47. Birkholtz, L.M., P. Alano, and D. Leroy, *Transmission-blocking drugs for malaria elimination.* Trends Parasitol, 2022. **38**(5): p. 390-403.
48. White, N.J., *Antimalarial drug resistance.* J Clin Invest, 2004. **113**(8): p. 1084-92.
49. Ng, C.L., et al., *CRISPR-Cas9-modified pfmdr1 protects Plasmodium falciparum asexual blood stages and gametocytes against a class of piperazine-containing compounds but potentiates artemisinin-based combination therapy partner drugs.* Mol Microbiol, 2016. **101**(3): p. 381-93.
50. Peatey, C.L., et al., *Effect of antimalarial drugs on Plasmodium falciparum gametocytes.* J Infect Dis, 2009. **200**(10): p. 1518-21.
51. Creek, D.J., et al., *Metabolomics-Based Screening of the Malaria Box Reveals both Novel and Established Mechanisms of Action.* Antimicrob Agents Chemother, 2016. **60**(11): p. 6650-6663.

52. Carolino, K. and E.A. Winzeler, *The antimalarial resistome - finding new drug targets and their modes of action.* Curr Opin Microbiol, 2020. **57**: p. 49-55.
53. Duffey, M., et al., *Assessing risks of Plasmodium falciparum resistance to select next-generation antimalarials.* Trends Parasitol, 2021. **37**(8): p. 709-721.
54. Reader, J., et al., *Multistage and transmission-blocking targeted antimalarials discovered from the open-source MMV Pandemic Response Box.* Nat Commun, 2021. **12**(1): p. 269.
55. Ramesh, R., et al., *Repurposing of a drug scaffold: Identification of novel sila analogues of rimonabant as potent antitubercular agents.* Eur J Med Chem, 2016. **122**: p. 723-730.
56. La Rosa, V., et al., *MmpL3 is the cellular target of the antitubercular pyrrole derivative BM212.* Antimicrob Agents Chemother, 2012. **56**(1): p. 324-31.
57. Deidda, D., et al., *Bactericidal activities of the pyrrole derivative BM212 against multidrug-resistant and intramacrophagic Mycobacterium tuberculosis strains.* Antimicrob Agents Chemother, 1998. **42**(11): p. 3035-7.
58. Xie, S., et al., *The endocannabinoid system and rimonabant: a new drug with a novel mechanism of action involving cannabinoid CB1 receptor antagonism--or inverse agonism--as potential obesity treatment and other therapeutic use.* J Clin Pharm Ther, 2007. **32**(3): p. 209-31.
59. Bolla, J.R., *Targeting MmpL3 for anti-tuberculosis drug development.* Biochem Soc Trans, 2020. **48**(4): p. 1463-1472.
60. Fotie, J., C.M. Matherne, and J.E. Wroblewski, *Silicon switch: Carbon-silicon Bioisosteric replacement as a strategy to modulate the selectivity, physicochemical, and drug-like properties in anticancer pharmacophores.* Chem Biol Drug Des, 2023. **102**(2): p. 235-254.
61. Fujii, S. and Y. Hashimoto, *Progress in the medicinal chemistry of silicon: C/Si exchange and beyond.* Future Med Chem, 2017. **9**(5): p. 485-505.
62. Cowell, A.N. and E.A. Winzeler, *Advances in omics-based methods to identify novel targets for malaria and other parasitic protozoan infections.* Genome Med, 2019. **11**(1): p. 63.
63. Cowell, A.N., et al., *Mapping the malaria parasite druggable genome by using in vitro evolution and chemogenomics.* Science, 2018. **359**(6372): p. 191-199.
64. Allman, E.L., et al., *Metabolomic Profiling of the Malaria Box Reveals Antimalarial Target Pathways.* Antimicrob Agents Chemother, 2016. **60**(11): p. 6635-6649.
65. Murithi, J.M., et al., *Combining Stage Specificity and Metabolomic Profiling to Advance Antimalarial Drug Discovery.* Cell Chem Biol, 2020. **27**(2): p. 158-171 e3.
66. Painter, H.J., et al., *Specific role of mitochondrial electron transport in blood-stage Plasmodium falciparum.* Nature, 2007. **446**(7131): p. 88-91.
67. Ke, H., et al., *Genetic investigation of tricarboxylic acid metabolism during the Plasmodium falciparum life cycle.* Cell Rep, 2015. **11**(1): p. 164-74.
68. Goodman, C.D., et al., *Parasites resistant to the antimalarial atovaquone fail to transmit by mosquitoes.* Science, 2016. **352**(6283): p. 349-53.
69. Sturm, A., et al., *Mitochondrial ATP synthase is dispensable in blood-stage Plasmodium berghei rodent malaria but essential in the mosquito phase.* Proc Natl Acad Sci U S A, 2015. **112**(33): p. 10216-23.
70. Matz, J.M., et al., *An Unusual Prohibitin Regulates Malaria Parasite Mitochondrial Membrane Potential.* Cell Rep, 2018. **23**(3): p. 756-767.
71. Kaiser, G., et al., *High resolution microscopy reveals an unusual architecture of the Plasmodium berghei endoplasmic reticulum.* Mol Microbiol, 2016. **102**(5): p. 775-791.
72. van Dooren, G.G., et al., *Development of the endoplasmic reticulum, mitochondrion and apicoplast during the asexual life cycle of Plasmodium falciparum.* Mol Microbiol, 2005. **57**(2): p. 405-19.
73. Striepen, B., et al., *Building the perfect parasite: cell division in apicomplexa.* PLoS Pathog, 2007. **3**(6): p. e78.
74. Sinden, R.E. and M.E. Smalley, *Gametocytogenesis of Plasmodium falciparum in vitro: the cell-cycle.* Parasitology, 1979. **79**(2): p. 277-96.
75. Li, J., et al., *Repurposing the mitotic machinery to drive cellular elongation and chromatin reorganisation in Plasmodium falciparum gametocytes.* Nat Commun, 2022. **13**(1): p. 5054.
76. Dearnley, M.K., et al., *Origin, composition, organization and function of the inner membrane complex of Plasmodium falciparum gametocytes.* J Cell Sci, 2012. **125**(Pt 8): p. 2053-63.

77. Goldberg, D.E. and J. Zimmerberg, *Hardly Vacuous: The Parasitophorous Vacuolar Membrane of Malaria Parasites.* Trends Parasitol, 2020. **36**(2): p. 138-146.
78. Lanfrancotti, A., et al., *Plasmodium falciparum: mRNA co-expression and protein co-localisation of two gene products upregulated in early gametocytes.* Exp Parasitol, 2007. **116**(4): p. 497-503.
79. Silvestrini, F., et al., *Genome-wide identification of genes upregulated at the onset of gametocytogenesis in Plasmodium falciparum.* Mol Biochem Parasitol, 2005. **143**(1): p. 100-10.
80. Varijakshi, G., et al., *Transcriptomic approaches for identifying potential transmission blocking vaccine candidates in Plasmodium falciparum: a review of current knowledge and future directions.* 3 Biotech, 2023. **13**(10): p. 344.
81. Gulati, S., et al., *Profiling the Essential Nature of Lipid Metabolism in Asexual Blood and Gametocyte Stages of Plasmodium falciparum.* Cell Host Microbe, 2015. **18**(3): p. 371-81.
82. Tran, P.N., et al., *Changes in lipid composition during sexual development of the malaria parasite Plasmodium falciparum.* Malar J, 2016. **15**: p. 73.
83. Bobenchik, A.M., et al., *Plasmodium falciparum phosphoethanolamine methyltransferase is essential for malaria transmission.* Proc Natl Acad Sci U S A, 2013. **110**(45): p. 18262-7.
84. Gonzalez-Bulnes, P., et al., *PG12, a phospholipid analog with potent antimalarial activity, inhibits Plasmodium falciparum CTP:phosphocholine cytidylyltransferase activity.* J Biol Chem, 2011. **286**(33): p. 28940-28947.
85. McNamara, C.W., et al., *Targeting Plasmodium PI(4)K to eliminate malaria.* Nature, 2013. **504**(7479): p. 248-253.
86. Matz, J.M., *Plasmodium's bottomless pit: properties and functions of the malaria parasite's digestive vacuole.* Trends Parasitol, 2022. **38**(7): p. 525-543.
87. Rosenthal, P.J. and S.R. Meshnick, *Hemoglobin catabolism and iron utilization by malaria parasites.* Mol Biochem Parasitol, 1996. **83**(2): p. 131-9.
88. Loria, P., et al., *Inhibition of the peroxidative degradation of haem as the basis of action of chloroquine and other quinoline antimalarials.* Biochem J, 1999. **339 (Pt 2)**(Pt 2): p. 363-70.
89. Campanale, N., et al., *Identification and characterization of heme-interacting proteins in the malaria parasite, Plasmodium falciparum.* J Biol Chem, 2003. **278**(30): p. 27354-61.
90. Slater, A.F. and A. Cerami, *Inhibition by chloroquine of a novel haem polymerase enzyme activity in malaria trophozoites.* Nature, 1992. **355**(6356): p. 167-9.
91. Sullivan, D.J., *Theories on malarial pigment formation and quinoline action.* Int J Parasitol, 2002. **32**(13): p. 1645-53.
92. Krugliak, M., J. Zhang, and H. Ginsburg, *Intraerythrocytic Plasmodium falciparum utilizes only a fraction of the amino acids derived from the digestion of host cell cytosol for the biosynthesis of its proteins.* Mol Biochem Parasitol, 2002. **119**(2): p. 249-56.
93. Lew, V.L., T. Tiffert, and H. Ginsburg, *Excess hemoglobin digestion and the osmotic stability of Plasmodium falciparum-infected red blood cells.* Blood, 2003. **101**(10): p. 4189-94.
94. Edgar, R.C.S., et al., *Methods Used to Investigate the Plasmodium falciparum Digestive Vacuole.* Front Cell Infect Microbiol, 2021. **11**: p. 829823.
95. Winstanley, P., *Modern chemotherapeutic options for malaria.* Lancet Infect Dis, 2001. **1**(4): p. 242-50.
96. Warhurst, D.C., J.C. Craig, and I.S. Adagu, *Lysosomes and drug resistance in malaria.* Lancet, 2002. **360**(9345): p. 1527-9.
97. Adams, C.L., et al., *Compound classification using image-based cellular phenotypes.* Methods Enzymol, 2006. **414**: p. 440-68.
98. Loo, L.H., L.F. Wu, and S.J. Altschuler, *Image-based multivariate profiling of drug responses from single cells.* Nat Methods, 2007. **4**(5): p. 445-53.
99. Young, D.W., et al., *Integrating high-content screening and ligand-target prediction to identify mechanism of action.* Nat Chem Biol, 2008. **4**(1): p. 59-68.
100. Ljosa, V., et al., *Comparison of methods for image-based profiling of cellular morphological responses to small-molecule treatment.* J Biomol Screen, 2013. **18**(10): p. 1321-9.
101. Reisen, F., et al., *Linking phenotypes and modes of action through high-content screen fingerprints.* Assay Drug Dev Technol, 2015. **13**(7): p. 415-27.
102. Sundaramurthy, V., et al., *Integration of chemical and RNAi multiparametric profiles identifies triggers of intracellular mycobacterial killing.* Cell Host Microbe, 2013. **13**(2): p. 129-42.

103. Castoreno, A.B., et al., *Small molecules discovered in a pathway screen target the Rho pathway in cytokinesis.* Nat Chem Biol, 2010. **6**(6): p. 457-63.
104. Loo, L.H., et al., *An approach for extensibly profiling the molecular states of cellular subpopulations.* Nat Methods, 2009. **6**(10): p. 759-65.
105. Futamura, Y., et al., *Morphobase, an encyclopedic cell morphology database, and its use for drug target identification.* Chem Biol, 2012. **19**(12): p. 1620-30.
106. Ziegler, S., S. Sievers, and H. Waldmann, *Morphological profiling of small molecules.* Cell Chem Biol, 2021. **28**(3): p. 300-319.
107. Grys, B.T., et al., *Machine learning and computer vision approaches for phenotypic profiling.* J Cell Biol, 2017. **216**(1): p. 65-71.
108. Bray, M.A., et al., *Cell Painting, a high-content image-based assay for morphological profiling using multiplexed fluorescent dyes.* Nat Protoc, 2016. **11**(9): p. 1757-74.
109. Charles River Laboratories. *Cell Painting Assay*. 2023; Available from: https://www.criver.com/products-services/discovery-services/screening-and-profiling-assays/high-content-imaging/cell-painting-assay?region=3701.
110. Way, G.P., et al., *Morphology and gene expression profiling provide complementary information for mapping cell state.* Cell Syst, 2022. **13**(11): p. 911-923 e9.
111. Hughes, R.E., et al., *Multiparametric High-Content Cell Painting Identifies Copper Ionophores as Selective Modulators of Esophageal Cancer Phenotypes.* ACS Chem Biol, 2022. **17**(7): p. 1876-1889.
112. Chandrasekaran, S.N., et al., *Image-based profiling for drug discovery: due for a machine-learning upgrade?* Nat Rev Drug Discov, 2021. **20**(2): p. 145-159.
113. Keiser, M.J., et al., *Relating protein pharmacology by ligand chemistry.* Nat Biotechnol, 2007. **25**(2): p. 197-206.
114. Jumper, J., et al., *Highly accurate protein structure prediction with AlphaFold.* Nature, 2021. **596**(7873): p. 583-589.
115. Varadi, M., et al., *AlphaFold Protein Structure Database: massively expanding the structural coverage of protein-sequence space with high-accuracy models.* Nucleic Acids Res, 2022. **50**(D1): p. D439-D444.
116. Friesner, R.A., et al., *Extra precision glide: docking and scoring incorporating a model of hydrophobic enclosure for protein-ligand complexes.* J Med Chem, 2006. **49**(21): p. 6177-96.
117. Trager, W. and J.B. Jensen, *Human malaria parasites in continuous culture. 1976.* J Parasitol, 2005. **91**(3): p. 484-6.
118. Allen, R.J. and K. Kirk, *The membrane potential of the intraerythrocytic malaria parasite Plasmodium falciparum.* J Biol Chem, 2004. **279**(12): p. 11264-72.
119. Allen, R.J. and K. Kirk, *Plasmodium falciparum culture: the benefits of shaking.* Mol Biochem Parasitol, 2010. **169**(1): p. 63-5.
120. Sun, W., et al., *Novel lead structures with both Plasmodium falciparum gametocytocidal and asexual blood stage activity identified from high throughput compound screening.* Malar J, 2017. **16**(1): p. 147.
121. van Biljon, R., et al., *Hierarchical transcriptional control regulates Plasmodium falciparum sexual differentiation.* BMC Genomics, 2019. **20**(1): p. 920.
122. Ngernna, S., et al., *Efficient synchronization of Plasmodium knowlesi in vitro cultures using guanidine hydrochloride.* Malar J, 2019. **18**(1): p. 148.
123. Trager, W., *What triggers the gametocyte pathway in Plasmodium falciparum?* Trends Parasitol, 2005. **21**(6): p. 262-4.
124. Reader, J., et al., *Nowhere to hide: interrogating different metabolic parameters of Plasmodium falciparum gametocytes in a transmission blocking drug discovery pipeline towards malaria elimination.* Malar J, 2015. **14**: p. 213.
125. Paquet, T., et al., *Antimalarial efficacy of MMV390048, an inhibitor of Plasmodium phosphatidylinositol 4-kinase.* Sci Transl Med, 2017. **9**(387).
126. Sivandzade, F., A. Bhalerao, and L. Cucullo, *Analysis of the Mitochondrial Membrane Potential Using the Cationic JC-1 Dye as a Sensitive Fluorescent Probe.* Bio Protoc, 2019. **9**(1).
127. Gunjan, S., et al., *Artemisinin Derivatives and Synthetic Trioxane Trigger Apoptotic Cell Death in Asexual Stages of Plasmodium.* Front Cell Infect Microbiol, 2018. **8**: p. 256.

128. Linzke, M., et al., *Live and Let Dye: Visualizing the Cellular Compartments of the Malaria Parasite Plasmodium falciparum.* Cytometry A, 2020. **97**(7): p. 694-705.
129. Hambrock, A., C. Loffler-Walz, and U. Quast, *Glibenclamide binding to sulphonylurea receptor subtypes: dependence on adenine nucleotides.* Br J Pharmacol, 2002. **136**(7): p. 995-1004.
130. Thakur, V., et al., *Eps15 homology domain containing protein of Plasmodium falciparum (PfEHD) associates with endocytosis and vesicular trafficking towards neutral lipid storage site.* Biochimica et Biophysica Acta (BBA) - Molecular Cell Research, 2015. **1853**(11, Part A): p. 2856-2869.
131. Tran, P.N., et al., *A female gametocyte-specific ABC transporter plays a role in lipid metabolism in the malaria parasite.* Nature Communications, 2014. **5**(1): p. 4773.
132. Dasaradhi, P.V.N., et al., *Food vacuole targeting and trafficking of falcipain-2, an important cysteine protease of human malaria parasite Plasmodium falciparum.* Molecular and Biochemical Parasitology, 2007. **156**(1): p. 12-23.
133. Howe, R., et al., *Isoprenoid biosynthesis inhibition disrupts Rab5 localization and food vacuolar integrity in Plasmodium falciparum.* Eukaryot Cell, 2013. **12**(2): p. 215-23.
134. Zhitomirsky, B., H. Farber, and Y.G. Assaraf, *LysoTracker and MitoTracker Red are transport substrates of P-glycoprotein: implications for anticancer drug design evading multidrug resistance.* J Cell Mol Med, 2018. **22**(4): p. 2131-2141.
135. Smilkstein, M., et al., *Simple and inexpensive fluorescence-based technique for high-throughput antimalarial drug screening.* Antimicrob Agents Chemother, 2004. **48**(5): p. 1803-6.
136. Bennett, T.N., et al., *Novel, rapid, and inexpensive cell-based quantification of antimalarial drug efficacy.* Antimicrob Agents Chemother, 2004. **48**(5): p. 1807-10.
137. Verlinden, B.K., et al., *Discovery of novel alkylated (bis)urea and (bis)thiourea polyamine analogues with potent antimalarial activities.* J Med Chem, 2011. **54**(19): p. 6624-33.
138. LaMonte, G.M., et al., *Pan-active imidazolopiperazine antimalarials target the Plasmodium falciparum intracellular secretory pathway.* Nat Commun, 2020. **11**(1): p. 1780.
139. The Plasmodium Genome Database, C., *PlasmoDB: An integrative database of the Plasmodium falciparum genome. Tools for accessing and analyzing finished and unfinished sequence data. The Plasmodium Genome Database Collaborative.* Nucleic Acids Res, 2001. **29**(1): p. 66-9.
140. Istvan, E.S., et al., *Plasmodium Niemann-Pick type C1-related protein is a druggable target required for parasite membrane homeostasis.* Elife, 2019. **8**.
141. Linares, M., et al., *Identifying rapidly parasiticidal anti-malarial drugs using a simple and reliable in vitro parasite viability fast assay.* Malar J, 2015. **14**: p. 441.
142. Lelievre, J., et al., *Activity of clinically relevant antimalarial drugs on Plasmodium falciparum mature gametocytes in an ATP bioluminescence "transmission blocking" assay.* PLoS One, 2012. **7**(4): p. e35019.
143. Posayapisit, N., et al., *Transgenic pyrimethamine-resistant plasmodium falciparum reveals transmission-blocking potency of P218, a novel antifolate candidate drug.* Int J Parasitol, 2021. **51**(8): p. 635-642.
144. Salcedo-Sora, J.E., et al., *The proliferating cell hypothesis: a metabolic framework for Plasmodium growth and development.* Trends Parasitol, 2014. **30**(4): p. 170-5.
145. MacRae, J.I., et al., *Mitochondrial metabolism of sexual and asexual blood stages of the malaria parasite Plasmodium falciparum.* BMC Biol, 2013. **11**: p. 67.
146. Krungkrai, J., P. Prapunwattana, and S.R. Krungkrai, *Ultrastructure and function of mitochondria in gametocytic stage of Plasmodium falciparum.* Parasite, 2000. **7**(1): p. 19-26.
147. Evers, F., et al., *Composition and stage dynamics of mitochondrial complexes in Plasmodium falciparum.* Nat Commun, 2021. **12**(1): p. 3820.
148. Okamoto, N., et al., *Apicoplast and mitochondrion in gametocytogenesis of Plasmodium falciparum.* Eukaryot Cell, 2009. **8**(1): p. 128-32.
149. Lamour, S.D., et al., *Changes in metabolic phenotypes of Plasmodium falciparum in vitro cultures during gametocyte development.* Malar J, 2014. **13**: p. 468.
150. Fisher, N., et al., *Cytochrome b mutation Y268S conferring atovaquone resistance phenotype in malaria parasite results in reduced parasite bc1 catalytic turnover and protein expression.* J Biol Chem, 2012. **287**(13): p. 9731-9741.

151. Crofts, A.R., *The cytochrome bc1 complex: function in the context of structure.* Annu Rev Physiol, 2004. **66**: p. 689-733.
152. Elokely, K.M. and R.J. Doerksen, *Docking challenge: protein sampling and molecular docking performance.* J Chem Inf Model, 2013. **53**(8): p. 1934-45.
153. Pantsar, T. and A. Poso, *Binding Affinity via Docking: Fact and Fiction.* Molecules, 2018. **23**(8).
154. Goldberg, D.E., *Complex nature of malaria parasite hemoglobin degradation [corrected].* Proc Natl Acad Sci U S A, 2013. **110**(14): p. 5283-4.
155. Kirkegaard, T. and M. Jaattela, *Lysosomal involvement in cell death and cancer.* Biochim Biophys Acta, 2009. **1793**(4): p. 746-54.
156. Boya, P. and G. Kroemer, *Lysosomal membrane permeabilization in cell death.* Oncogene, 2008. **27**(50): p. 6434-51.
157. Wang, F., R. Gomez-Sintes, and P. Boya, *Lysosomal membrane permeabilization and cell death.* Traffic, 2018. **19**(12): p. 918-931.
158. Ch'ng, J.H., et al., *Drug-induced permeabilization of parasite's digestive vacuole is a key trigger of programmed cell death in Plasmodium falciparum.* Cell Death Dis, 2011. **2**(10): p. e216.